

30261



National Library of Canada

Bibliothèque nationale du Canada

CANADIAN THESES ON MICROFICHE

THÈSES CANADIENNES SUR MICROFICHE

NAME OF AUTHOR/NOM DE L'AUTEUR MR. RALPH P. DANYLUK

TITLE OF THESIS/TITRE DE LA THÈSE Energy Transport in Photosynthesis

UNIVERSITY/UNIVERSITÉ Simon Fraser University

DEGREE FOR WHICH THESIS WAS PRESENTED/ GRADE POUR LEQUEL CETTE THÈSE FUT PRÉSENTÉE M. Sc.

YEAR THIS DEGREE CONFERRED/ANNÉE D'OBTENTION DE CE GRADE 1976

NAME OF SUPERVISOR/NOM DU DIRECTEUR DE THÈSE K. Colbow, Associate Professor of Physics

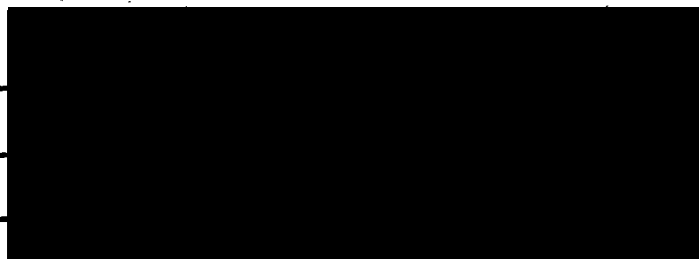
Permission is hereby granted to the NATIONAL LIBRARY OF CANADA to microfilm this thesis and to lend or sell copies of the film.

L'autorisation est, par la présente, accordée à la BIBLIOTHÈQUE NATIONALE DU CANADA de microfilmer cette thèse et de prêter ou de vendre des exemplaires du film.

The author reserves other publication rights, and neither the thesis nor extensive extracts from it may be printed or otherwise reproduced without the author's written permission.

L'auteur se réserve les autres droits de publication; ni la thèse ni de longs extraits de celle-ci ne doivent être imprimés ou autrement reproduits sans l'autorisation écrite de l'auteur.

DATED/DATÉ Aug. 12/75 SIGNED/SIGNÉ.

PERMANENT ADDRESS/RÉSIDENCE FIXÉ 

INFORMATION TO USERS

THIS DISSERTATION HAS BEEN
MICROFILMED EXACTLY AS RECEIVED

This copy was produced from a microfiche copy of the original document. The quality of the copy is heavily dependent upon the quality of the original thesis submitted for microfilming. Every effort has been made to ensure the highest quality of reproduction possible.

PLEASE NOTE: Some pages may have indistinct print. Filmed as received.

Canadian Theses Division
Cataloguing Branch
National Library of Canada
Ottawa, Canada K1A 0N4

AVIS AUX USAGERS

LA THESE A ETE MICROFILMEE
TELLE QUE NOUS L'AVONS RECUE

Cette copie a été faite à partir d'une microfiche du document original. La qualité de la copie dépend grandement de la qualité de la thèse soumise pour le microfilmage. Nous avons tout fait pour assurer une qualité supérieure de reproduction.

NOTA BENE: La qualité d'impression de certaines pages peut laisser à désirer. Microfilmée telle que nous l'avons reçue.

Division des thèses canadiennes
Direction du catalogage
Bibliothèque nationale du Canada
Ottawa, Canada K1A 0N4

ENERGY TRANSPORT IN PHOTOSYNTHESIS

by

RALPH PETER DANYLUK

B.Sc., University of Manitoba, 1971

A THESIS SUBMITTED IN PARTIAL FULFILLMENT OF

THE REQUIREMENTS FOR THE DEGREE OF

MASTER OF SCIENCE

in the Department

of

Physics

C

RALPH PETER DANYLUK 1975

SIMON FRASER UNIVERSITY

August 1975

All rights reserved. This thesis may not be reproduced
in whole or in part, by photocopy or other means, with-
out permission of the author.

APPROVAL

Name: Ralph Peter Danyluk
Degree: Master of Science
Title of Thesis: Energy Transport in Photosynthesis

Examining Committee:

Chairman: J. C. Irwin

K. Colbow
Senior Supervisor

A. S. Arrott

B. L. Jones

R. R. Parsons
Assistant Professor of Physics
University of British Columbia

Date Approved: Aug 11/75

PARTIAL COPYRIGHT LICENSE

I hereby grant to Simon Fraser University the right to lend my thesis or dissertation (the title of which is shown below) to users of the Simon Fraser University Library, and to make partial or single copies only for such users or in response to a request from the library of any other university, or other educational institution, on its own behalf or for one of its users. I further agree that permission for multiple copying of this thesis for scholarly purposes may be granted by me or the Dean of Graduate Studies. It is understood that copying or publication of this thesis for financial gain shall not be allowed without my written permission.

Title of Thesis/Dissertation:

Energy Transport in Photosynthesis

Author:

(signature)

MR. RALPH P. DANYLUK

(name)

Aug. 12/75

(date)

ABSTRACT

A theoretical model is presented to account for the physical mechanism of energy transfer from antenna molecules to the reaction centers in photosynthesis. The energy transfer is described by a generalized transport equation or "master equation". The solution of this equation for the proposed model gives a relationship between the antennae interaction energy and the transfer rate. The results are shown to be in agreement with inter-antenna transfer rates calculated from experimental fluorescence lifetimes. Previous theories were based either on the Förster mechanism, which is valid for very small interaction energies, or an exciton model valid for very large interactions, but experimental results seemed to indicate that the actual situation was intermediate between these two. The Förster theory and the exciton model are shown to be limiting cases of the master equation. We show that the solution of the master equation provides a useful formulation for the calculation of energy transfer rates over a wide range of interaction strengths.

ACKNOWLEDGEMENTS

I would like to thank Dr. K. Colbow and Dr. U. Schreiber for their help and encouragement with this thesis.

I would also like to thank Dr. A. S. Arrott, Dr. W. Wattamaniuk, Dr. K. Millard, Dr. B. Jones, and other members of the SFU physics department for their support and encouragement.

Greatly appreciated is the fine work and willingly help of the SFU audio visual department.

TABLE OF CONTENTS

ABSTRACT.....	iii
ACKNOWLEDGEMENTS.....	iv
LIST OF ILLUSTRATIONS.....	vii
I. INTRODUCTION TO PHOTOSYNTHESIS.....	1
II. A MODEL OF THE PHOTOSYNTHETIC UNIT	
i) membrane structure and pigments.....	8
ii) the chlorophyll-a molecule.....	9
iii) orientation of chlorophyll-a.....	12
iv) mean-spacing of chlorophyll-a.....	14
v) number of antenna molecules.....	15
vi) the reaction center.....	16
vii) summary of model assumptions.....	21
III. EXCITATION TRANSFER IN MOLECULAR SYSTEMS	
i) classification of molecular interaction.....	22
ii) strong interaction.....	24
iii) weak interaction.....	32
iv) very-weak interaction.....	34
v) Förster equation.....	38

IV. MASTER EQUATION APPROACH TO EXCITATION TRANSFER

i) introduction to master equations.....	41
ii) Pauli master equation.....	43
iii) generalized master equation.....	44
iv) memory function for molecular systems.....	47
v) solution of the generalized master equation.....	55
vi) summary.....	68

V. APPLICATION TO THE PHOTOSYNTHETIC UNIT

i) "in vitro" absorption spectra of chl-a.....	69
ii) applying the generalized master equation....	77
iii) the "in vivo" absorption spectrum of chlorophyll.....	88
iv) conclusions.....	92

BIBLIOGRAPHY.....	93
-------------------	----

APPENDICES

A. Derivation of the Förster Equation.....	96
B. Derivation of the Generalized Master Equation.....	106
C. Derivation of the Memory Function for Molecular Transitions.....	115
D. The orientation factor.....	121
E. Derivation of the wave equation from the master equation.....	125

LIST OF ILLUSTRATIONS

<u>Figure</u>		<u>Page</u>
1.	The time scale of photosynthesis.....	3
2.	The anatomy of a chloroplast.....	4
3.	Flow chart of the "light-reaction" in photosynthesis.....	5
4.	Lipid bilayer model of the cell membrane.....	9
5.	The chlorophyll-a molecule.....	11
6.	Excitation intensity dependence of the fluorescence lifetime.....	20
7.	Franck-Condon diagram.....	23
8.	Summary of energy transfer mechanisms.....	40
9.	Memory function.....	53
10.	Solution of the master equation.....	64
11.	R dependence of transfer rate from the master equation solution.....	67
12.	Absorption spectrum of chlorophyll-a.....	71
13.	Gaussian and Lorentzian fit of the red absorption band of chlorophyll-a.....	72
14.	Memory function for single and double Gaussian components.....	74
15.	Transfer rate vs. interaction energy from the master equation solution.....	76
16.	Interaction energy vs. chl-a separation.....	85
	Table of the summary of results.....	87

I: INTRODUCTION TO PHOTOSYNTHESIS

In photosynthesis light is collected by an array of "antenna molecules", usually some form of chlorophyll, and then transferred to one of two reaction centers. There are about 300 antenna chlorophyll for each reaction center in plants*. This energy transfer process takes place in the order of a nanosecond. At the molecular level a nanosecond is a significant period of time when one considers that about 10,000 molecular vibrations take place in this interval.

The set of antennae associated with each active reaction center is called a photosynthetic unit (PSU).

After the energy is trapped by one kind of reaction center (center II), the resulting excited state of the trap is used to oxidize water and the electron is transported to another reaction center (center I) where it is used to reduce NADP^+ (oxidized nicotin- amide-adenine dinucleotide phosphate) to NADPH, after absorption of a further photon. NADPH in conjunction with ATP is then utilized in the reduction of carbon dioxide to carbohydrate. This last step, called the Calvin cycle, takes place in the absence of light on a much longer time scale.

* Bacteria have only one reaction center with about 50 antenna bacteriochlorophyll per center.

About 97% of the light quanta are transferred to a reaction center. Most of the remaining 3% which is not utilized photochemically is given off as fluorescence.

Fig. 1 illustrates the major time divisions in photosynthesis. Two major divisions are indicated: the so-called "light and dark reactions." The former includes the trapping of energy by the reaction center and the production of oxidizing-reducing agents. The latter is involved with the production of carbohydrate (Calvin cycle), and free oxygen, the end results of photosynthesis.

Fig. 3 outlines the main steps in the light reaction of photosynthesis.

In eucaryotic cells the photosynthetic apparatus is localized in cellular bodies called chloroplasts. These are ellipsoidal in shape, 3 to 10 microns in length and 1 1/2 microns thick. Chloroplasts are surrounded by a continuous outer membrane. Inside is a system of flattened vesicles called thylakoid disks, which are usually arranged in stacks called grana. This is illustrated in Fig. 2. The light reaction takes place in the thylakoid membranes, while the dark reaction takes place in the surrounding cytoplasm inside the chloroplast.

Evidence that there are two kinds of reaction centers or photosystems comes from studies of the quantum efficiency of photosynthesis in plant cells as a function of the wavelength of incident light, measured by O₂ evolution. Although the efficiency is uniform over

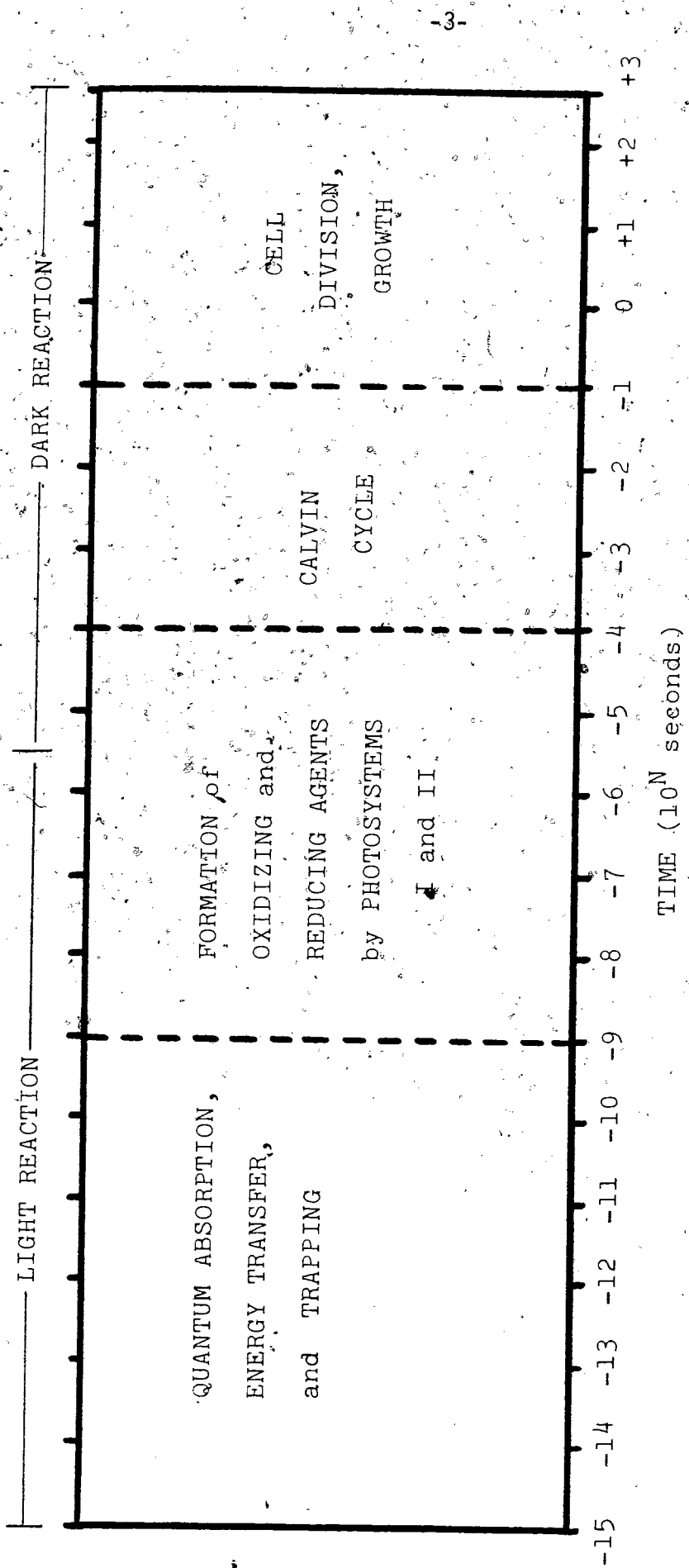


Fig. 1 The duration of the major processes in photosynthesis

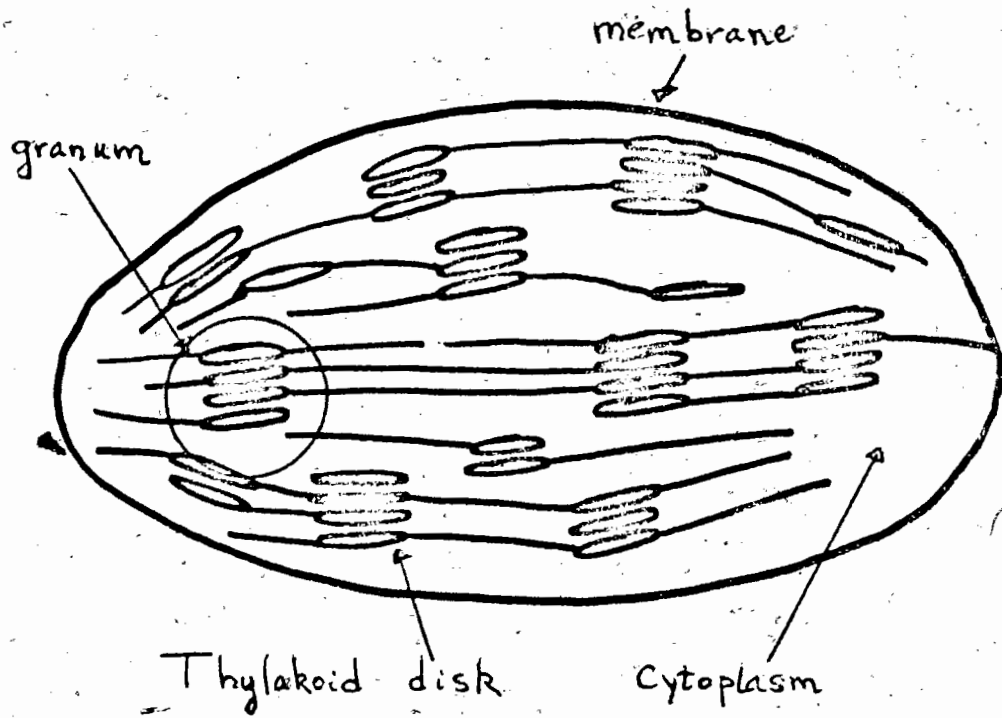
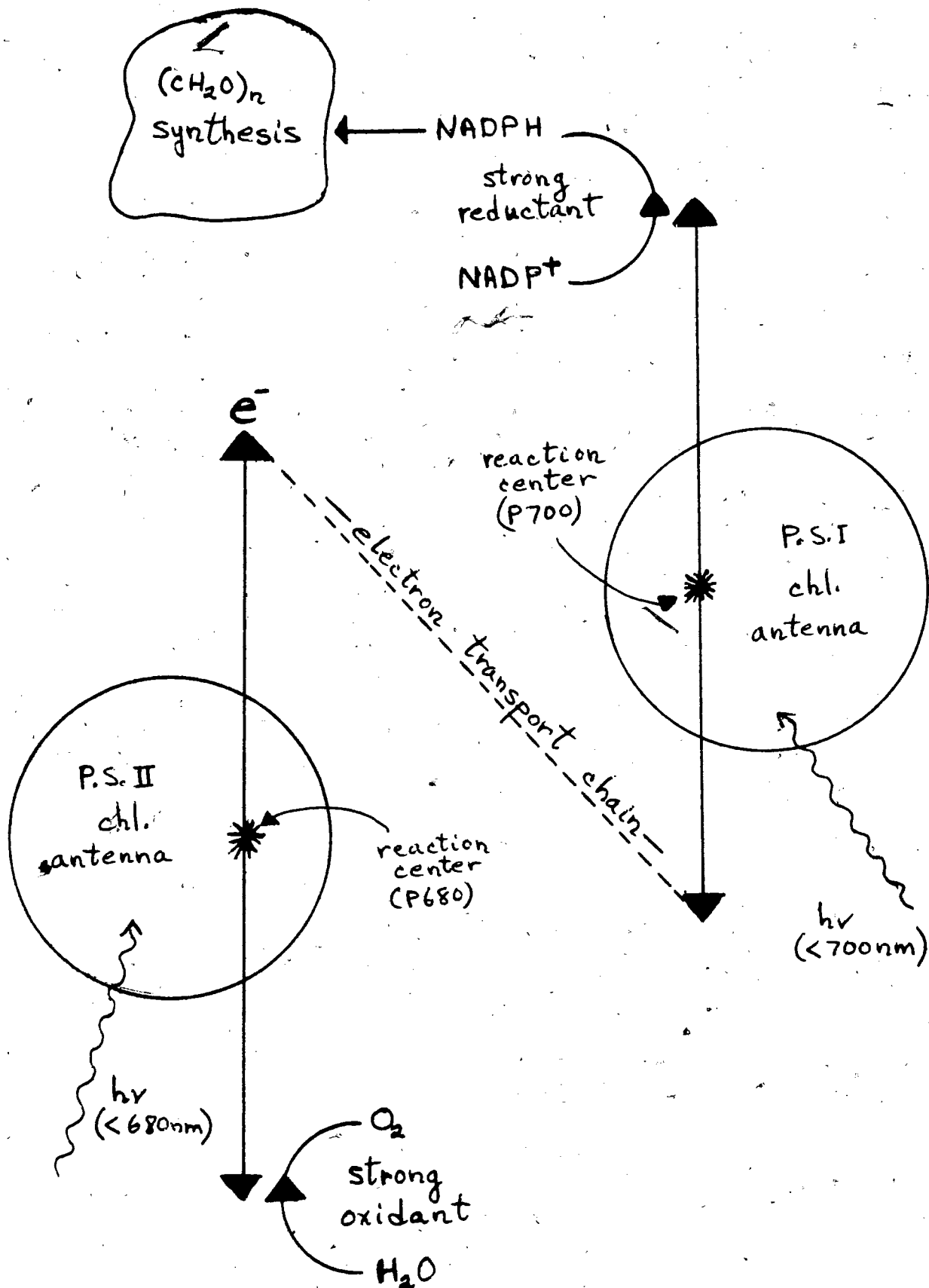


Fig. 2 The anatomy of a chloroplast

Fig. 3 Simplified flow chart of the "light reaction" in photosynthesis.



most of the spectrum, it drops significantly in the red at wavelengths of 680 nm and above. It was shown by Emerson around 1957 that if the far-red light is supplemented with light of a shorter wavelength; i.e. 650 nm light, the quantum efficiency of oxygen production is substantially higher than the average of the sum of the production from the separate beams. The enhancement of the efficiency of the far-red light by simultaneous illumination with shorter wavelength light is known as the Emerson effect. These findings suggested that two different light reactions are involved. Four photons absorbed by photosystem II result in the splitting of two water molecules into four hydrogen ions and one oxygen molecule. Photosystem I also traps four photons in the production of the two NADPH molecules from the electrons produced by the water splitting. Thus eight photons are involved in photosynthesis leading to the evolution of one oxygen molecule.

In 1932, Emerson and Arnold, using short pulses of incident light found a point was reached where the amount of oxygen evolved did not increase with further increases in flash intensity. They determined that at the saturation point one oxygen molecule was given off per 2400 chlorophyll molecules. Interpreting this in terms of the two photosystems means 600 chlorophylls are divided amongst the two photosystems. The pulse width of the flashes must be short enough for each reaction center to be only utilized once ($< 10^{-5}$ second). The pulse repetition rate must also be small enough to allow the dark enzymatic reaction to be completed and the photosynthetic apparatus to recover which is about one pulse per second.

The reaction centers are not yet fully understood. They are designated in green plants as P700 for the reaction center of photosystem I, and P680 for reaction center II, because of light induced changes in the "in vivo" absorption spectrum observed at these wavelengths. They are thought to be chlorophyll-protein complexes.

Detailed discussions of the two reaction centers, photosynthetic units, and the chemistry of photosynthesis can be found in the books by: Rabinowitch and Govindjee (1969), Clayton (1965, 1972, 1971) and the articles: (Levine, 1969), (Govindjee, 1974).

Excellent electron micrographs and more details of the anatomical structure of chloroplasts (the cellular bodies which house the PSU's) can be found in the book by O.V.S. Heath (1969).

This thesis will concern itself with the transfer of energy from the antenna chlorophyll to the trap.

II. A MODEL OF THE PHOTOSYNTHETIC UNIT

i) membrane structure and pigments

The model of the PSU that we will be using is illustrated in Fig. 4. It consists of an array of chlorophyll molecules embedded in a fluid lipid bilayer membrane. We will also assume that the lipids and the globular proteins in the membrane have little influence on energy transfer between chlorophyll molecules other than by acting as a medium of uniform index of refraction, and providing a thermal bath (Katz, 1973).

We will consider the antenna chlorophyll as being of one type, chlorophyll-a (chl-a). Other pigments such as chlorophyll-b, carotenoids, and phycobilins are also present in green plants and algae. These pigments absorb light at shorter wavelengths and pass the energy almost irreversibly to the chl-a antennae. In this way they serve to extend the absorption spectrum of the plant over most of the visible region. The antenna chl-a can then be excited either by direct absorption or by energy transfer from these other pigments. It has also been shown that fluorescence from photosystem II is independent of the exciting wavelength in the emission spectrum suggesting that the fluorescence "is due to a single species of chl-a molecules...." (Müller et al. 1969; Goedheer, 1972). We will discuss PSU fluorescence in section vi. In bacteria, bacteriochlorophyll does the analogous work of chl-a.

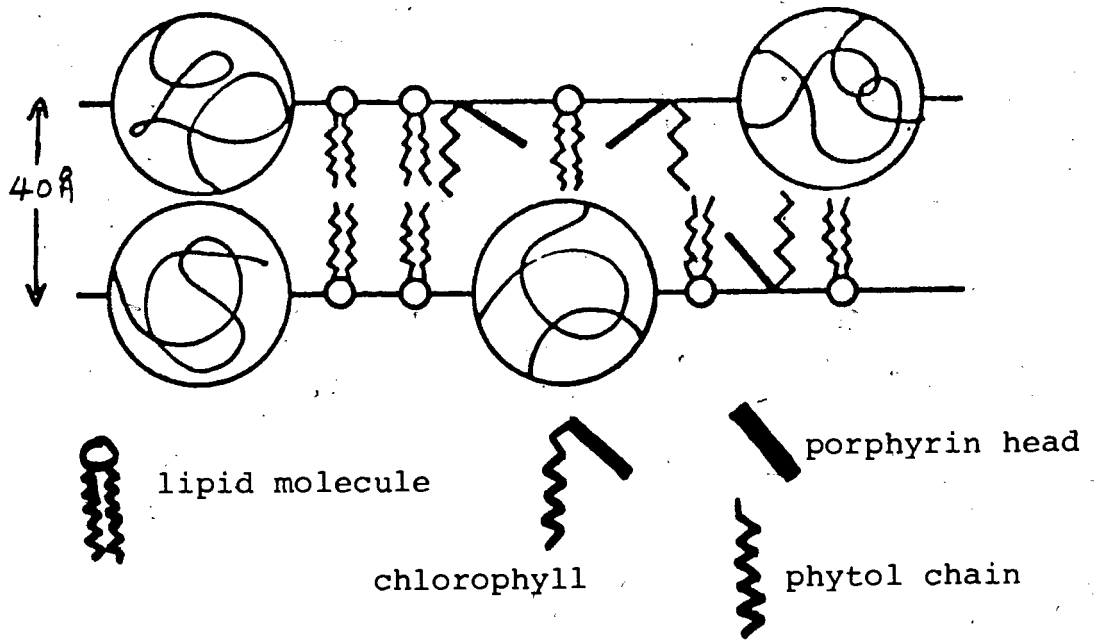


Fig. 4 Lipid bilayer model. The lipid molecules form bilayer 40Å thick. The coiled up spherical proteins (60Å diameter) are immersed about 20Å into the lipid. The chlorophyll molecules with their porphyrin head make an angle of 48° to the membrane surface and their phytol chains are perpendicular to the surface.

The lipid-protein membrane is essentially transparent at optical wavelengths and will be assigned an average real index of refraction of $n = 1.45$ (Bay and Pearlstein, 1963; Pearlstein, 1964), the refractive index of lipid-like materials.

ii) the chl-a molecule

The chl-a molecule is shown in Fig. 5. The porphyrin head is a chromophore responsible for light absorption in the visible. The long hydrocarbon phytol chain is transparent at optical wavelengths. The porphyrin head is free to move at the point designated by the dotted line just below the C = O bond. Chl-a has two main absorption bands, in the red and blue regions. The transition dipole moments for these bands are oriented perpendicular to each other in the porphyrin plane along the dotted lines in Fig. 5. We will return to a more detailed discussion of the absorption spectrum in Section V. We are primarily interested in structural details at this point.

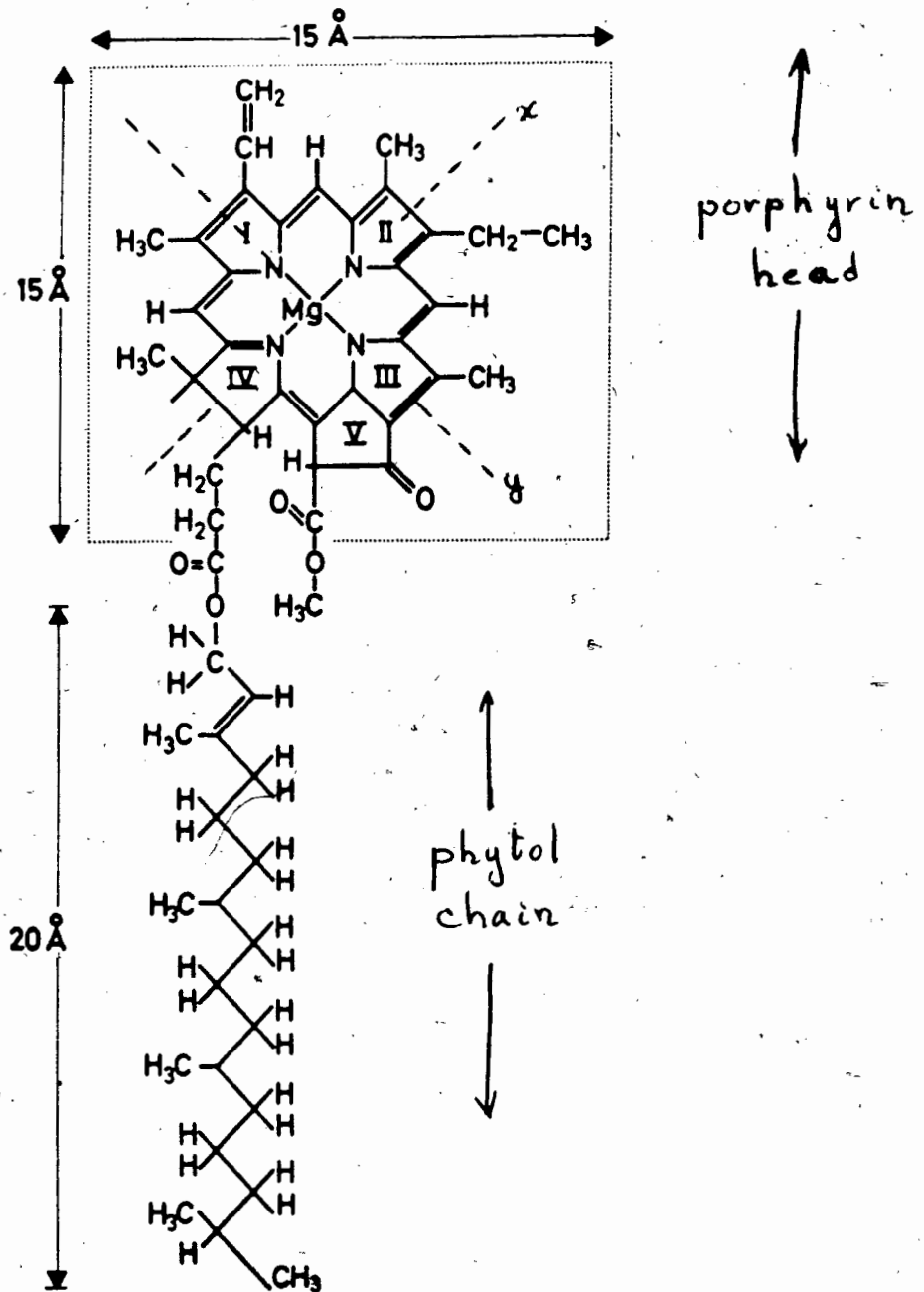


Fig. 5 Structure of chl-a. The molecule is believed to be anchored by the group V (cyclopentanone ring) to the water-lipid interface; the red transition moment points from ring I to III, along the y-axis, and makes an angle of 35° with the membrane surface.

iii) orientation of chl-a in the membrane

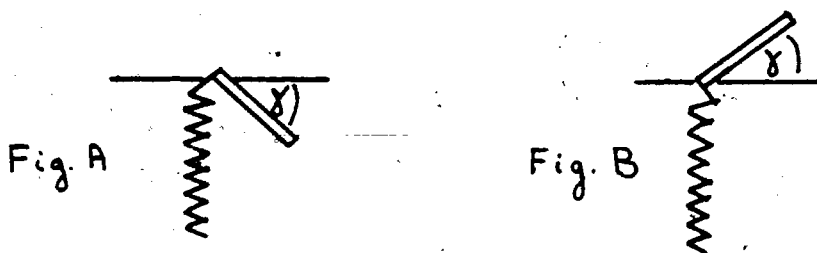
The spectrum of chl-a "in vivo" is more complex than that of chl-a in dilute solution. Instead of one main band at about 660 nm in solution, a band with components at 673, 683, and 695nm is observed in vivo (Clayton, 1965; Kreutz, 1970). We will return to the discussion of the "in vivo" spectrum in chapter VI. What is important for our consideration of chl-a orientation is that the dichroism of the "in vivo" spectrum is very weak except for the 693 component, i.e. the dichroic ratio is approximately one.

Dichroic ratio D, is defined as the ratio of the absorbance for vertically polarized light to that for horizontally polarized light. The measurement of dichroism is one of the main techniques for determining molecular orientation.

A dichroic ratio of one "in vivo" would imply random orientation of the porphyrin rings in the membrane. However, Kreutz(1970) has argued that the only way to obtain this value and still have the chl-a anchored by the phytol chain in the membrane is to have the red and blue transition moments at an angle of 35.3° with the membrane plane, but free to rotate azimuthally. Then with the red and blue transitions at right angles to each other, the plane of the porphyrin head is inclined at an angle of 54.7° to the membrane plane (Kreutz, 1970). Direct measurements of chl-a orientation in artificial

membranes have also been made. Using lipid bilayers, Steinemann et al. (1972) measured the red transition moment as being oriented at $35^\circ \pm 2^\circ$ to the membrane plane and the blue transition moment at $26^\circ \pm 3^\circ$ to the membrane plane (these are averaged values for three different lipids). They determined the inclination of the porphyrin plane as being $46 \pm 5^\circ$ to the membrane surface. About the same time, Cherry et al. (1971) did similar measurements with lipid bilayers and determined that the red and blue transition moments of chl-a make angles of 36.5° and 26° respectively, to the membrane surface. Using the assumption that transition moments are perpendicular, they deduced that the plane of the ring is inclined at 48° to the membrane surface. Hoff (1974) using lecithin multilayers measured the orientation of the red transition moment as $34.3 \pm 1.1^\circ$ to the membrane and the inclination of the porphyrin plane as $55.4 \pm 1^\circ$ with the membrane plane. We will use an average value of $35 \pm 2^\circ$ for the angle of the red transition moment with the membrane plane. The inclination of the porphyrin plane will not enter into our calculations.

Steinemann in his paper also argues that the porphyrin head is in the hydrocarbon region of the membrane rather than in the polar region. i.e. Fig. A rather than Fig. B.



This information cannot be deduced from dichroism measurements.

The argument is based on the fact that the larger part of the porphyrin ring is hydrophobic except for the $-\text{COOCH}_3$ and C = O groups of the cyclopentanone ring (Fig. 5) which should make contact with the water-lipid interface.

iv) mean-spacing of the chl-a antennae

Wolken and Schwertz (1953) using electron microscopy measured an available area of 222 and 246 \AA^2 per chlorophyll molecule in the chloroplasts of "Euglena Gracilis" and "Poteriochronmonas stipitata." Kreutz (1970) using X-ray diffraction measured an area of $2.8 \times 10^4 \text{\AA}^2$ for 128 chlorophyll molecules giving an average of 215 \AA^2 per chlorophyll. Thomas et al. (Thomas, Minnaert and Elbers, 1965) using electron microscopy measured a range of 90 to 360 \AA^2 per chlorophyll for grana-bearing chloroplasts. Their average is 240 \AA^2 per chlorophyll. For our model we choose a range of 200 to 250 \AA^2 corresponding to a mean-spacing of $15 \pm 1 \text{\AA}$ between chlorophyll molecules (Colbow, 1973).

v) Number of Antenna Molecules

The next thing we need to know in our model is the number of antenna chlorophyll associated with a trap. In Section I we discussed the Emerson and Arnold experiment which showed that 2400 chlorophyll molecules were involved in the evolution of one oxygen molecule. Eight photons were needed in this process, according to the two photosystem concept. This gives us a value of about 300 chl-a per reaction center, assuming an even division between photosystem I and II. However, in the literature one sometimes finds lower values being used without justification, such as 100 (Borisov and Ilna, 1973). Schmid and Gaffron have recently repeated the Emerson and Arnold experiment measuring the amount of $C^{14}O_2$ fixed per saturating flash (Schmid and Gaffron, 1968, 1969, 1971). They vindicated the value of 2400 for normal, healthy plants, but showed that the size of the PSU could vary in discrete steps of 300 chlorophyll around the value of 2400. This may be due to inactive reaction centers. In chlorophyll deficient mutants, units as small as 1/8 of this value were found. In chlorophyll-rich adult plants and algae most of the unit sizes were between 2000 and 2700. Therefore considering the variability of unit size and the uncertainty in partitioning of the antenna chlorophylls between the two photosystems, we have chosen to consider a range of 250 to 350 antenna chl-a per reaction center in our model calculations.

vi) the trap or reaction center

Excitation in the PSU can either be trapped by a reaction center or lost as fluorescence. Interconversion processes such as singlet to triplet transitions leading to non-radiative de-excitation in the antenna chlorophyll are considered to be negligible. The quantum efficiency and lifetime of fluorescence following a pulse of absorbed light are the main experimental measurements in the investigation of energy transfer in the PSU

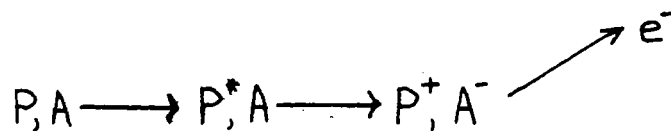
Changes in fluorescence, induced by affecting the operation of the reaction centers and the electron carrier chain, using pressure, chemicals, changes in oxygen concentration, light pulses, etc., are used to study the light reaction of photosynthesis. They are often made under a steady-state light bias, which determines a base fluorescence level, before any of the induced changes. The fluorescence lifetime measurements that we refer to are made by observing the decay of fluorescence after an initial short pulse of light. Fluorescence induction measurements are made over periods in the order of seconds, while fluorescence lifetime measurements are of the order of nanoseconds.

The trap is essentially a potential well, and in this model is considered as irreversible, i.e. energy once trapped does not return

to the antenna chlorophyll. This is borne out "in vivo" by the fact that the trap absorbs light directly at a longer wavelength (lower energy) than the antenna chl-a, 680 nm for PSII (Katz, 1973). Hoch and Knox (1968) estimate a value of 10^{-4} for the ratio of out to in jump probabilities.

The trap itself is believed to be a specialized form of Chl-a, designated here as "P" (following Clayton, 1972), aggregated with a protein. In reaction center II, "P" is associated with an unidentified substance Z acting as an electron donor and an electron acceptor Q, possibly a quinone. The "P" of reaction center I is probably associated with plastocyanin and an electron acceptor which is possibly a pteridine-protein complex (Clayton, 1971; Govindjee, 1974). In the following, we will outline a possible trapping mechanism. The electron acceptor associated with the chlorophyll, P, will be designated as "A".

P could receive an excitation quantum from the antenna pigments and then donate an electron to A:



where P^* denotes P in the singlet excited state. The restoration of the state "P,A" must be completed before the reaction center can

perform its function again. We say that the trap is "open" in the state P,A but closed in any of the states P⁺,A; P,A⁻; or P⁺,A⁻.

When all the traps are open the fluorescence from the antenna pigments is at a minimum as the traps compete with fluorescence for the excitation and thus quench the fluorescence. With the trap closed the fluorescence would be maximum. This hypothesis has been borne out by experiment.

With the traps "open" the decay time of fluorescence (as measured by pulse fluorimetry) would be the same as the time needed for the excitation to reach the trap. This condition is obtained experimentally by using low light levels (no saturation). Thus we make the identification between the unsaturated fluorescence lifetime measured experimentally τ_F and the trapping time τ_T . i.e. $\tau_F = \tau_T$

Müller et al. (1969) have shown that the fluorescence lifetime reaches limiting values for both high and low light intensities. We reproduce here one of their curves demonstrating this for "Chlorella", Fig. 6. The saturation value is 1.92 nsec. while the lifetime approaches a value of about 0.35 nsec. for low light intensity. These findings are consistent with the assumed mechanism in which energy absorbed by chl-a is transferred to the trapping centers by a

singlet state resonance mechanism. After receiving a quantum the traps are unable to accept energy until they have completed the photochemical process. In the limit of very low light intensity the traps are unoccupied on the average, so the excitation quanta are trapped very rapidly resulting in a short fluorescence lifetime. At high light intensity, or under condition of chemically poisoned traps, the traps are occupied or not functional, so that excitation resides in the bulk chlorophyll for longer periods of time, resulting in increased fluorescence lifetime. Thus the open-trap situation corresponds to the fluorescence lifetime measurements at very low light intensities.

The five-fold increase of fluorescence with light intensity is strong evidence that a considerable part of the energy is delivered to the traps via singlet excited states. If the energy transfer was by triplet states, little fluorescence increase would be expected, as fluorescence is the result of radiative decay of singlet energy levels (Borisov and Godik, 1973; Borisov and I'lna, 1973).

Measurements of fluorescence lifetime prior to Müller et al. were done at unspecified excitation intensities and the results range in value from 0.6 to 1.7 nsec. (Müller et al., 1969). Müller argues that the limiting values were not observed because no consideration was given to the level of the exciting intensity.

They also conclude that the saturating value appears to be universal in plants. The "open-trap" value is also the same for blue and red algae (Goedheer, 1972). We will adopt the value of 0.4 ± 0.1 nsec. as the "open-trap" fluorescence lifetime and interpret it as the trapping time of excitation.

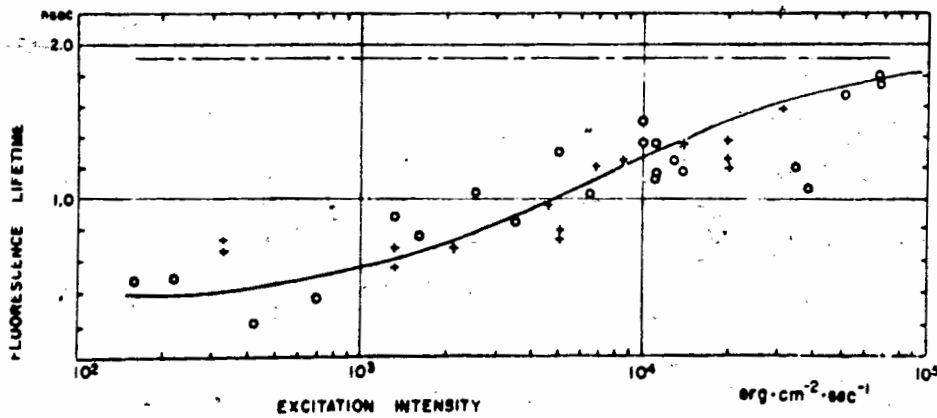


Fig. 6 Excitation intensity dependence of the fluorescence lifetime of "Chlorella". From Müller et. al. (1969)

What we have described applies only to PSII. The fluorescence from PSI decays about ten times faster than PSII and only recently have accurate measurements been made (Alfano and Seibert, 1974; Borisov and I'lna, 1973). There also seems to be an absence of fluorescence that varies with the state of the traps in PSI, and it has been suggested that energy transfer takes place via triplet states (Borisov and I'lna, 1973; Clayton, 1972). In short, the behaviour of PSI is not as well understood as that of PSII.

vii) summary of model assumptions

We have described a model for photosystem II of plant photosynthetic units. It incorporates the following assumptions based on the experimental work described in this section.

i) the chl-a molecules are randomly distributed and make an angle of $35^\circ \pm 2^\circ$ with the membrane plane. They have a mean spacing of $15 \pm 1 \text{ \AA}$

ii) there are 250 to 350 antenna chlorophyll

iii) the trapped excitation energy does not escape

iv) the lipids and proteins have no effect on energy transfer except to provide an environment of constant temperature and refractive index.

v) all the antenna molecules are chl-a

vi) the fluorescence lifetime is 0.4 ± 0.1 nsec.

III. EXCITATION TRANSFER

1) classification of molecular interaction strength

We will begin by reviewing the theory of intermolecular interaction.

Fig. 8 illustrates an energy level diagram (Franck-Condon diagram) for a molecule. Only the ground state and the first-excited state with its vibrational levels are shown.

Two parameters are important for a discussion of inter-molecular interaction strength. The first is the width of the electronic band, sometimes called the Franck-Condon bandwidth, symbolized by ΔE . It determines the width of the entire band system of the spectra of an isolated molecule as well as the Stokes shift between the absorption and emission bands. ΔE has an energy value of about 3000 cm^{-1} ($\sim 0.3 \text{ eV}$), and is of the same order of magnitude as the energy of the vibrational quanta, about 1000 cm^{-1} (Forster, 1967). The second parameter is the vibrational band-width $\Delta E'$, and is of the order of 10 to 30 cm^{-1} .

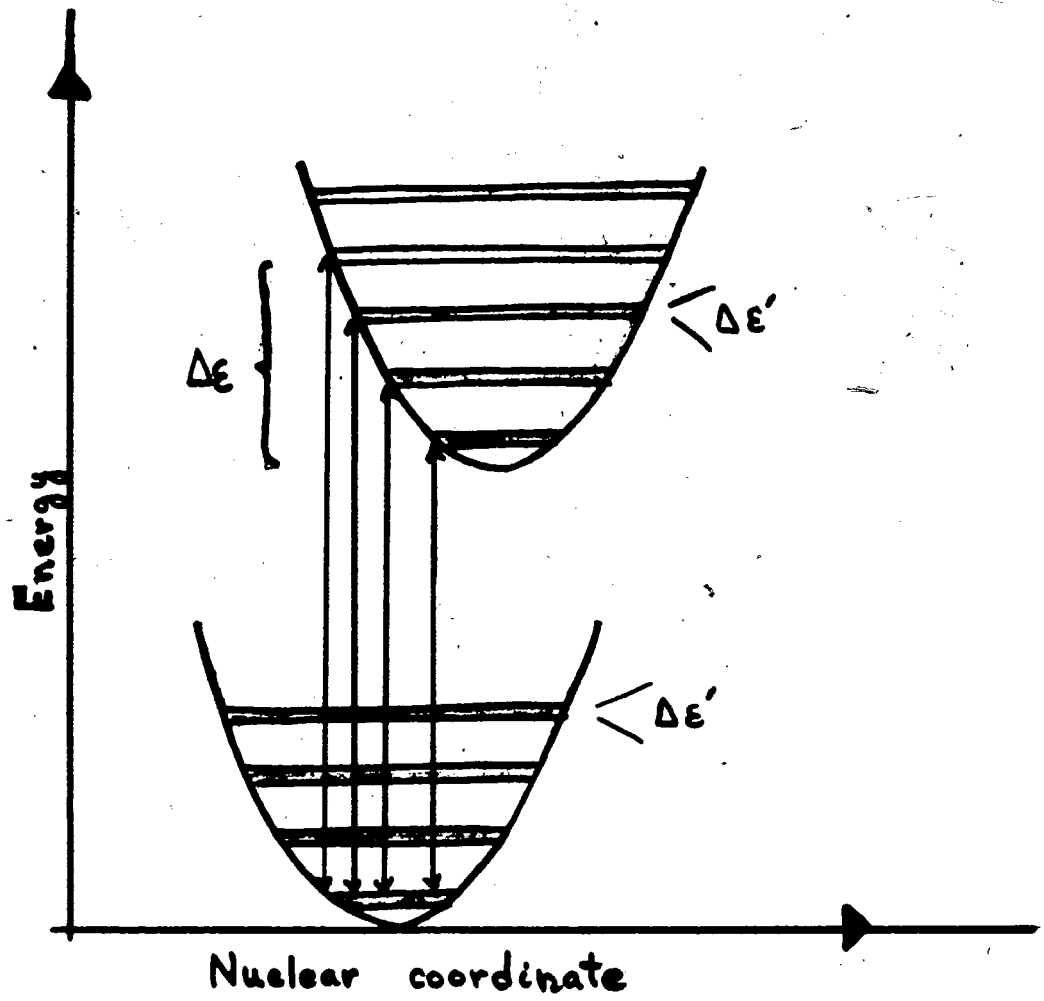


Fig. 7 "Franck-Condon" diagram for a diatomic molecule, illustrating the electronic band-width, ΔE , and vibrational band-width, $\Delta E'$

With these two parameters we can define three cases of coupling strength:

- i) $|u| \gg \Delta E \gg \Delta E'$ strong
- ii) $\Delta E \gg |u| \gg \Delta E'$ weak or intermediate
- iii) $\Delta E \gg \Delta E' \gg |u|$ very weak

$|u|$ is the absolute value of the interaction energy.

For a semi-quantitative derivation of these coupling strength criteria, see Simpson and Peterson (1957).

ii) Strong coupling:

In this case the intermolecular interaction energy is greater than vibrational energy levels within the individual molecules. The transfer of excitation occurs very quickly before any essential nuclear motion can take place (Born-Oppenheimer approximation). In strong coupling the situation may be described as follows:

If we have an array of N identical molecules and one of them is excited, our system is N-fold degenerate because we have N possible wavefunctions of the form: $\phi_n = \psi_n^* \prod_i' \psi_i$ all with the same eigenvalue. ψ_n^* is the wavefunction of the excited molecule, and ψ_i are the ground state wavefunctions. However, the interaction energy $|u|$ acts as a perturbation and "splits" the degeneracy. A set of stationary state eigenfunctions for the perturbed Hamiltonian can be written in the form:

$$\begin{aligned}\Phi_1 &= \phi_1 + \phi_2 + \dots + \phi_N \\ \Phi_2 &= \phi_1 - \phi_2 + \dots + \phi_N \\ &\vdots \\ \Phi_n &= \phi_1 - \phi_2 - \dots - \phi_N\end{aligned}$$

Each stationary state involves excitation of all molecules. Thus the excitation is considered as being delocalized. Time dependent states can be constructed from the stationary ones which behave as coherent waves of excitation which sweep across the lattice.

The above description is termed the molecular exciton concept, and arises out of the resonance with neighbouring identical molecules. The exciton migrates with constant group velocity (Franck and Teller, 1938). Also what has been said applies only for ideal crystals. Impurities, lattice imperfections, and thermal degeneration lead to scattering or absorption of excitons into many k states by exciton-phonon interaction. Thus the coherence of the exciton is decreased so that the propagation becomes more diffusive than wave-like. The root-mean-square displacement is then proportional to the square root of time rather than directly to time as with the wave-like exciton.

Strongly coupled systems have absorption spectra which differ markedly from the single component spectra. Absorption bands are split by the exciton interaction.

We will now consider a dimer (two molecules strongly coupled) and calculate the transfer rate of excitation from one to the other.

Our derivation follows Förster's (1965). The Hamiltonian for the dimer is

$$H = H_a + H_b + V_{ab} \quad (1)$$

where V_{ab} is the interaction potential.

The eigenfunctions of the unperturbed Hamiltonian, $V_{ab} = 0$, are

$\phi'_a \phi_b$ or $\phi_a \phi'_b$, where the prime indicates the excited states.

The interaction potential couples the two possible states of the system so that we can then write the eigenfunctions as linear combinations:

$$\Phi_+ = (\cos\alpha) \phi'_a \phi_b + (\sin\alpha) \phi_a \phi'_b \quad (2)$$

$$\Phi_- = (\sin\alpha) \phi_a \phi'_b - (\cos\alpha) \phi_a \phi'_b \quad (3)$$

The coefficients, \cos and \sin , are chosen so that Φ_+ and Φ_- are orthonormal. The parameter α , however, remains arbitrary and depends on the strength of V_{ab} . If $V_{ab} = 0$ then α will be 0, or $\pi/2$, giving $\Phi_+ = \phi'_a \phi_b$ and $\Phi_- = \phi_a \phi'_b$. We shall presently show that when V_{ab} is greater than the bandwidth ΔE , α becomes $\pi/4$. This gives:

$$\Phi_{\pm} = \frac{1}{\sqrt{2}} (\phi'_a \phi_b + \phi_a \phi'_b)$$

A similar result is obtained with two interacting fermions. Eqns 2 and 3 are stationary state solutions. Now we will consider the time dependent problem; the time evolution of the system from $\phi'_a \phi_b$ to $\phi_a \phi'_b$, which is the rate of energy transfer from molecules "a" excited and "b" unexcited, to "a" unexcited and "b" excited.

We wish to solve the following eigenvalue equation:

$$\langle \Phi_j | H | \Phi_i \rangle = W_i \delta_{ij} \quad (4)$$

In order to specify α , it is sufficient to solve the equation:

$$\langle \Phi_+ | H | \Phi_- \rangle = 0 \quad (5)$$

Direct substitution of Eqns 1, 2, and 3 into 5 gives:

$$(\sin^2 \alpha - \cos^2 \alpha) U + \{W_{a'b} - W_{ab'}\} \cos \alpha \sin \alpha = 0 \quad (6)$$

Here U is the resonance integral $\langle a'b | V_{ab} | ab' \rangle$ and $W_{a'b}$ is the integral $\langle a'b | H | a'b \rangle$ which is the total energy of the configuration $\phi'_a \phi_b$:

$$W_{a'b} = W_a' + W_b' + V_{a'b} \quad (7)$$

Similarly for $W_{ab'} = W_a + W_b + V_{ab'}$

and finally

$$\tan \alpha = \frac{2U}{(W_{a'b} - W_{ab'})} ; \quad 0 \leq \alpha \leq \pi/2 \quad (8)$$

Having specified α we can solve for the eigenvalues:

$$\langle \Phi_{\pm} | H | \Phi_{\pm} \rangle = W_{\pm} \quad (9)$$

Direct substitution results in:

$$W_{\pm} = \cos^2 \alpha W_{a'b} + \sin^2 \alpha W_{ab'} + \sin 2\alpha U \quad (10)$$

There are two limiting cases: i) $2|u| \ll |W_{a'b} - W_{ab'}|$; $\alpha = 0$ or $\pi/2$
with $\alpha = 0$, we have:

$$\begin{aligned} \Phi_+ &= \phi_{a'} \phi_b & \Phi_- &= \phi_a \phi_{b'} \\ W_+ &= W_{a'b} & W_- &= W_{ab'} \end{aligned} \quad (11)$$

With $\alpha = \pi/2$ the situation is reversed. The excitation is essentially localized on one molecule or the other, and corresponds to the very weak coupling case.

case ii): $2|u| \gg |W_{a'b} - W_{ab'}|$; $\alpha = \pi/4$

$$\begin{aligned} \Phi_{\pm} &= \frac{1}{\sqrt{2}} (\phi_{a'} \phi_b \pm \phi_a \phi_{b'}) \\ W_{\pm} &= \frac{1}{2} (W_{a'b} + W_{ab'}) \pm u \end{aligned} \quad (12)$$

This is the resonance, strong coupling case, where the wave functions are the symmetric and anti-symmetric combinations of the locally excited (unperturbed) configurations. The excitation is distributed equally over both molecules. The energies of the two exciton states differ by $2u$, which is called the exciton splitting energy.

We can now write the time dependent wave function as:

$$\psi_{\pm}(t) = \Phi_{\pm} e^{-iW_{\pm}t/\hbar} \quad (13)$$

and in general write the following linear combination:

$$\psi(t) = c_+ \Phi_+ e^{-iW_+t/\hbar} + c_- \Phi_- e^{-iW_-t/\hbar} \quad (14)$$

For $W_+ = W_-$ this represents a back and forth oscillation of the excitation between both molecules. If at $t = 0$ we assume molecule "a" only to be excited, then from Eqs. 2 and 3 we must have that

$$c_+ = \cos\alpha \quad \text{and} \quad c_- = \sin\alpha \quad (15)$$

By direct substitution of eqns 2, 3 and 10, 15 into eqn 14 we get:

$$\psi(t) = e^{-i\frac{1}{2}(W_+ + W_-)t/\hbar} \left[\left\{ \cos\left(\frac{Ut}{\hbar \sin 2\alpha}\right) - i \cos 2\alpha \cdot \sin\left(\frac{Ut}{\hbar \sin 2\alpha}\right) \right\} \phi'_a \phi_b - i \sin 2\alpha \sin\left(\frac{Ut}{\hbar \sin 2\alpha}\right) \phi_a \phi'_b \right] \quad (16)$$

Next we want to calculate the expectation value of the state $\phi_a \phi'_b$

From Eqn 16 we get

$$P_{ab'}(t) \equiv \langle ab' | ab' \rangle = \sin^2 2\alpha \sin^2 \left(\frac{Ut}{\hbar \sin 2\alpha} \right) \quad (17)$$

The maximum value of $f_{ab'}(t)$ is

$$f_{ab'}^{\max} = \sin^2 2\alpha \equiv \frac{\tan^2 2\alpha}{1 + \tan^2 2\alpha} = \frac{4U^2}{(W_{ab} - W_{ab'})^2 + 4U^2} \quad (18)$$

where we have substituted Eqn 7. $f_{ab'}^{\max}$ becomes large only when $\alpha \approx \pi/4$, that is, near resonance condition. To find the time, t_{\max} , at which $f_{ab'}^{\max}$ occurs, we set the first time derivative of Eqn 17 to zero and solve for t .

$$t^{\max} = \frac{\pi \hbar}{2|u|} \sin 2\alpha \quad (19)$$

We define the transfer rate, $\eta_{a \rightarrow b}$ as the maximum expectation value, $f_{ab'}^{\max}$, divided by t^{\max} and obtain

$$\eta_{a \rightarrow b} \equiv \frac{f_{ab'}^{\max}}{t^{\max}} = \frac{2|u|}{\pi \hbar} \sin 2\alpha \quad (20)$$

For strong coupling $\alpha = \pi/4$, therefore the transfer rate is:

$$\eta_{a \rightarrow b} = \frac{2|u|}{\pi \hbar} = \frac{4|u|}{\hbar} \quad (21)$$

Which agrees with what one might expect from the uncertainty principle:

$$\frac{1}{\Delta t} \leq \frac{\Delta E}{\hbar} \quad (22)$$

If our interaction $|u|$ is dipole-dipole in nature, then $|u| \propto R^{-3}$ and from Eqn 21 we see that $\eta_{a \rightarrow b} \propto R^{-3}$.

iii) weak coupling:

When the intermolecular interaction is intermediate between that of the electronic and vibrational energies, the coupling is called weak. Here only pairs of vibronic levels are at resonance with each other. One can proceed as before and describe the system by its stationary vibronic exciton states. Crudely speaking the transfer rate, $\eta_{a \rightarrow b}$, will then be described by Eqn 21 multiplied by the Franck-Condon integral of the intramolecular transition between vibrational levels: v and w .

$$\eta_{v,w} \approx \frac{4|u|}{h} S_{v,w}^2 \quad (23)$$

S_{vw} is the overlap integral of the wave functions of the vibrational levels v , w and is related to the intensity of transition. The product US_{vw} may be regarded as the interaction energy between the vibronic transitions of molecules a and b .

Although in an ideal crystal the vibronic exciton migrates with a constant group velocity, it moves more slowly according to Eqn 16. However, because of the sharper resonance condition, this coherent propagation is more sensitive to lattice irregularities and phonons. This leads to exciton-phonon scattering which rapidly diffuses the motion of the exciton after a few lattice distances.

This consideration will be important for our model later on. A detailed analysis of the weak coupling case is difficult because the usual Born-Oppenheimer separation of nuclear and electronic motion is not valid (Merrifield, 1963).

The changes in the absorption spectra of the monomer molecule are less drastic. The vibrational envelope is essentially retained and the individual vibrational bands are split in what is called Davydov splitting.

iv) Very-weak coupling:

In weak coupling we ignored the width of the vibrational bands assuming them to be reasonably sharp. If the interaction energy is of the order of the vibrational bandwidth, $\Delta E'$, we have the third case of very-weak coupling. Thus, two coinciding levels are not completely at resonance but only portions of them are.

If the coupling is so weak that transfer has not been accomplished during the lifetime of the vibronic level, the transfer will necessarily be affected by collision and vibrational energy exchange with the surroundings such as with phonons. This leads to the establishment of thermal equilibrium between the vibrational levels of an excited molecule and its surroundings. Such times are of the order 10^{-12} sec corresponding to a bandwidth of 30 cm^{-1} as mentioned earlier.

From Eqn 17 we have:

$$P_{ab'}(t) = \sin^2(2\alpha) \sin^2\left(\frac{U_{vw}t}{\hbar \sin 2\alpha}\right) ; U_{vw} \equiv U S_{vw}^2 \quad (24)$$

for the probability of energy exchange between vibrational level v of molecule a and w of molecule b . For small time this is :

$$P_{ab'}(t) \approx \frac{U_{vw}^2 t^2}{\hbar^2} \quad (25)$$

If a collision occurs at $t = \tau$ then $f_{a,b'}$ will have increased by an amount of:

$$\Delta f_{ab'} \approx \frac{U_{rw}^2 \tau^2}{h^2}$$

Such a collision will destroy all phase relations between the wavefunctions of "a" and "b", so that the increase in the next time interval between collisions will be:

$$f_{ab'}(t) \approx \frac{t}{\tau} \Delta f_{ab'} \approx \frac{U_{rw}^2 \tau}{h^2} t$$

where τ is the mean time between collisions. The transfer rate as defined before is then:

$$n_{a \rightarrow b'} \approx \frac{U_{rw}^2 \tau}{h^2} \quad (\tau \text{ is a constant})$$

The transfer rate is thus proportional to the square of the interaction energy as opposed to the first power as in the strong and weak case. If we express τ by the corresponding bandwidth $\Delta E = h/\tau$ we get:

$$n_{a \rightarrow b'} \approx \frac{4\pi^2 U_{rw}^2}{h \Delta E} \quad (26)$$

Very weak coupling leads to no recognizable changes in the absorption spectrum.

In the very-weak case the excitation is essentially localized on one molecule. Individual transfers are uncorrelated and the resulting energy propagation is completely diffusive.

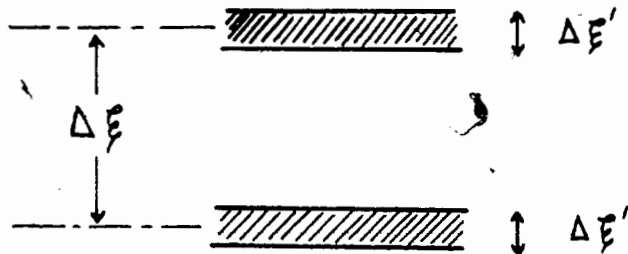
Diffusive motion of the excitation is Markoffian in nature. This means each step is independent of the past. Diffusion problems and random walk problems are isomorphic (Knapp, 1965) and we will make use of this fact later in developing our model of the motion of excitation in the PSU.

For molecules with continuous spectra or those which show little or no vibronic structure, the weak coupling region is non-existent, and the mechanism of energy transfer goes essentially from very weak to strong. This can be shown as follows:

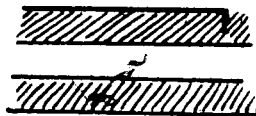
Consider the criteria for weak coupling,

$$\Delta E > |u| > \Delta E'$$

where ΔE is at its smallest the energy between two vibrational levels, and $\Delta E'$ is the width of the levels:



If the density of the levels becomes large or $\Delta E'$ becomes large so that the energy level picture looks like:



then ΔE can be of the same energy as $\Delta E'$. Therefore, the weak coupling criteria, is in effect, "squeezed-out". That is, $\Delta E \approx \Delta E'$, so that $|u|$ is either greater than ΔE or less than $\Delta E'$ so that if $|u|$ becomes larger than that required for very weak coupling, it is already large enough to produce the strong interaction.

Thus for polyatomic molecules, solutions, and many crystalline states, the weak interaction region is very small. We will see a quantitative example of this later in regard to our PSU model. The master equation approach to energy transfer, which we will develop in the next section, will allow us to prescribe a width to the intermediate region of weak coupling. It is thus possible for the very-weak coupling to give rise to a rate of energy transfer that is faster than the thermal relaxation rate, $1/\tau_{\text{relax}}$.

From Eqn 26 we see that if $|u|$ is dipole-dipole, $u \propto 1/R^3$, then the transfer rate for very-weak coupling is proportional to $1/R^6$.

The very-weak coupling mechanism is sometimes referred to as "inductive resonance transfer" meaning that a transition charge distribution is induced in a neighbouring molecule by the near-zone electric field of the oscillating charge distribution of the excited molecule.

v) the Förster equation

In the case where the excited state of the donor molecule has come to thermal equilibrium before transferring energy, the very-weak mechanism is called the Förster mechanism and is described by the Förster equation. The Förster equation is basically Eqn 26 written in terms of measurable spectral parameters such as the intensity and shape of the absorption and fluorescence bands.

One assumes a dipole-dipole interaction, a Boltzmann distribution of vibrational states (thermal equilibrium approximation), and with the Einstein relations for absorption and spontaneous emission, one obtains:

$$\eta_{a \rightarrow b} = \frac{1}{\tau_0} \frac{1}{R_{ab}^6} \left(\frac{9k^2 (\ln 10)}{128 \pi^5 n^4 N} \right) \int_0^{\infty} f(\nu) \xi(\nu) \frac{d\nu}{\nu^4} \quad (27)$$

where: ν = wave numbers (cm^{-1})

$\epsilon(\nu)$ = molar decadic extinction coefficient

$I(\nu)$ = fluorescence spectrum, normalized quanta/ cm^{-1}

N = number of molecules per millimole

n = index of refraction

τ_0 = natural fluorescence lifetime of an isolated molecule

k = factor representing the orientation of the dipoles

R = distance between the dipoles

Eqn 27 can be written as:

$$\eta_{a \rightarrow b} = \frac{1}{\tau_0} \left(\frac{R_0}{R} \right)^6 \quad (28)$$

where R^6 is defined from Eqn 27.

The details of the derivation of Eqn 27 are given in Appendix A.

Eqn 27 applies only to pairwise interactions with $\eta_{a \rightarrow b}$ the pairwise transfer rate. In a lattice the presence of more than one nearest neighbour will affect $\eta_{a \rightarrow b}$ in such a way as to increase the transition probability. Thus the actual transfer rate will be $\eta_B = \eta_{a \rightarrow b} \times B$ where B is the number of nearest neighbours (Bay and Pearlstein, 1963).

Fig. 8 Summary of the characteristics of the intermolecular transfer of excitation energy. τ_j is the nearest neighbour transfer time, $|u|$ is the interaction energy, R is the intermolecular spacing, λ is the exciting wavelength. (adapted from Clayton, 1965)

TRANSFER MECHANISM	DESCRIPTION	RANGE OF APPLICABILITY				DEPENDENCE OF TRANSFER RATE, τ_j , ON		
		τ_j (sec.)	$ u $ (cm^{-1})	R (\AA)	R	λ	T	
fast	delocalized molecular exciton	$< 3 \times 10^{-14}$	> 1000	< 5	R^{-3}	—	—	
weak	delocalized molecular (vibronic) exciton	3×10^{-14} to 3×10^{-12}	10 to 1000	5 to 20	R^{-3}	slight	slight	
very weak	localized inductive resonance transfer	3×10^{-12} to 3×10^{-8}	0.1 to 10	20 to 100	R^{-6}	—	moderate	

5

IV. THE MASTER EQUATION APPROACH

1) introduction to master equations

We have seen that there are three classes of strengths for intermolecular interaction and each has its own observable effects on the absorption spectra of the free molecule. The calculation of transfer rate in terms of interaction energy, U , using only well defined spectral parameters has been fully formulated only for the Forster case. The weak case has traditionally proved very difficult primarily because the Born-Oppenheimer separability of nuclear and electronic motion is not in general valid (Merrifield, 1963). In the strong case, direct measurement of the transfer rate in terms of coupling energy is not as yet experimentally possible. Strong coupling effects are usually studied by observing the splitting of spectral lines (Hochstrasser and Kasha, 1964).

Knox and Kenkre have developed a unified approach based on a "generalized master equation" that allows one to calculate the transfer rate in terms of interaction energy over a wide range of coupling strengths. This relationship is given in terms of well-defined spectral properties of the isolated molecule, such as half-width of the absorption band and the Stokes shift. The strong and very-weak coupling cases are readily obtained in the appropriate limits of the master-equation solution, while a continuous relationship between transfer rate and interaction energy is provided

throughout the intermediate weak region. We will first discuss the principles involved and derive the appropriate relationships. Then it will be applied to the model of the PSU previously discussed. Our goal is to come up with a figure giving the range of possible interaction energies between chl-a molecules in the PSU based on experimentally measured quantities such as the fluorescence lifetime, number of chlorophyll in the PSU, orientation and mean spacing.

In statistical mechanics the approach of a quantum system to statistical equilibrium under the influence of a perturbation is described by a particular kind of transport equation called a master equation. It is a relationship about the time evolution of quantum states in terms of transition probabilities between these states. It is called a master equation to distinguish it from transport equations of the Boltzmann type used in kinetic theory of gases.

First we will discuss the Pauli master equation which holds only for lowest order in the perturbation between states. We shall see that it is a good description of the very-weak coupling case, but is not applicable when the coupling is much stronger. A generalized master equation will then be discussed which is good to all orders of the perturbation. We will finally go on to show how this generalized master equation can be used to describe the transport of excitation in the PSU.

ii) the Pauli master equation

The Pauli Master Equation (PME) is:

$$dP_i(t)/dt = \sum_j [F_{ij} P_j(t) - F_{ji} P_i(t)]$$

It describes the evolution of the probability of excitation at a molecule P_i as a function of the probabilities of excitation at the other molecules (P_j) and the transition probability rates F_{ij} . The equation is Markoffian in nature, meaning that the probability, F_{ij} , of excitation jumping from i to j is independent of its previous location. In other words, memory of previous locations is lost. This is applicable to our model only in the case of very-weak energy coupling where the Forster mechanism is applicable. In this case the excitation can be considered as localized on a particular site and hops from one site to the next. The jump times would then be given by the Förster formulation and the trapping time could then be worked out by solving the set of coupled PME Eqns for the array of molecules (Knox, 1968).

The Markoffian PME is however, equivalent to a random walk. Montroll has worked out analytic equations for random walks in one, two, three dimensions and the results are essentially the same as those obtained from the PME.

Colbow (1973) has applied this Markoffian model to the PSU using the Forster formulation and Montroll's random walk equations. This was based on a mean-spacing of 15A and on new measurements for $R_0=65A$. The results were just larger than the thermal relaxation time. This would justify the use of the Forster' formulation, However the results were sufficiently close to the intermediate region to warrant a closer look. The energy transfer may take place sufficiently fast so that there is doubt about the applicability of the Förster equation (Borisov and I'lna, 1973; Seibert and Alfano, 1974).

iii) generalized master equations

We will now proceed to develop a single expression based on a single definition of transfer rate which will contain the strong and very weak regions as limits and ascribe a width to the intermediate region. The first step is to generalize the PME as follows (Knox and Kenkre, 1974):

$$\frac{dP_i(t)}{dt} = \int_0^t ds \sum_j \{ w_{ij}(t-s) P_j(s) - w_{ji}(t-s) P_i(s) \}$$

Here the transition probabilities are time dependent. The probability of transition depends on time less than t, i.e.) on where the excitation was before t. w_{ij} connects the probability at a site j at time s in the past to the rate change of probability at site i at the

present time t . This equation is non-Markoffian and is called the Generalized Master Equation (GME).

By substituting:

$$w_{ij}(t-s) = F_{ij} \delta(t-s)$$

into the GME one immediately obtains the PME. The delta function means that the transition probability depends on what happens at time t , not on any previous history. The PME thus eliminates the possibility of exciton or reversible resonance coupling between molecules.

Here we present a physical rationale for generalizing the PME; a more rigorous derivation of the GME is found in Appendix B, based on Liouville's equation for the density matrix of the system.

A useful approximation in our case is to assume that the time dependence of w_{ij} is independent of the sites i and j :

$$w_{ij}(t) = F_{ij} \phi(t) \tag{1}$$

where $\phi(t)$ is a time-dependent coefficient. The GME then reduces to:

$$dP_i(t)/dt = \int_0^t ds \phi(t-s) [\sum_j (F_{ij}P_j(s) - F_{ji}P_i(s))] \tag{2}$$

We will call $\phi(t)$ the memory function. The nature of the energy transfer is thus determined by $\phi(t)$ as well as by the rates F_{ij} .

It is illustrative at this point to show that both wave-like (coherent excitons) and diffusion (Markoffian, random walk) behaviour arise quite naturally from limiting forms of the GME.

If we make a nearest neighbour approximation and assume a continuum of sites, Eqn 2 can be written as: (Kenkre and Knox, 1974)

$$\frac{\partial P(x,t)}{\partial t} = \int_0^t ds Q(t-s) \frac{\partial^2 P(x,s)}{\partial x^2}$$

(see Appendix E for details of derivation) If we set: $Q(t) = c^2\Theta(t)$ where $\Theta(t)$ is the step function, we obtain the wave equation:

$$\frac{\partial^2 P(x,t)}{\partial t^2} = c^2 \frac{\partial^2 P(x,t)}{\partial x^2}$$

and if we set $Q(t) = D\delta(t)$ we get the diffusion equation:

$$\frac{\partial P(x,t)}{\partial t} = D \frac{\partial^2 P(x,t)}{\partial x^2}$$

The content of the wave and diffusion equations can be combined as the "telegrapher's" equation:

$$\frac{\partial^2 P(x,t)}{\partial t^2} + \frac{c^2}{D} \frac{\partial P(x,t)}{\partial t} = c^2 \frac{\partial^2 P(x,t)}{\partial x^2}$$

which is obtained from the GME by letting

$$Q(t) = c^2 e^{-(c^2/D)t}$$

a form intermediate between that of $\Theta(t)$ and $\delta(t)$.

iv) the memory function for molecular transitions

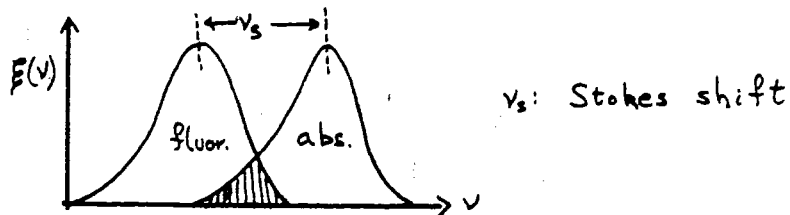
$\phi(t)$ defines the extent in time in which the process can be considered non-Markoffian. What we now need is a prescription for calculating $\phi(t)$. For molecular transitions, Kenkre and Knox (1974) derive the following expression for $\phi(t)$ in terms of Förster's equation: (Appendix C)

$$\phi(t) = [1/\pi f(0)] \int_{-\infty}^{\infty} f(\Delta\nu) \cos(\Delta\nu t) d(\Delta\nu) \quad (3)$$

where $f(0)$ is the Förster rate equation for two molecules given in terms of the overlap of their fluorescence and absorption curves:

$$f(0) \propto 1/R^6 \int_0^{\infty} [\xi(\nu)\xi(2\nu_0 - \nu)/\nu(2\nu_0 - \nu)] d\nu$$

where $\xi(\nu)$ is the extinction coefficient and ν_0 is the average of the absorption and fluorescence maximum.



$f(\Delta\nu)$ is given by the same equation as $f(0)$ but the peaks are shifted on the frequency scale by $+\Delta\nu/2$ for the emission and $-\Delta\nu/2$ for the absorption

Physically this would represent a molecule that has not come to full thermal equilibrium before transferring energy (thermal equilibrium would imply the full Stokes shift ν_s).

Gueron et al. (1967) considered the case of total overlap in formulating their "before-relaxation, very-weak coupling" case.

If the peaks are symmetrical or nearly so, the denominator is equal to ν_0 and can be removed from the integral.

We may write

$$f(0) = K \int_0^{\infty} \mathcal{E}(\nu) \mathcal{E}(2\nu_0 - \nu) d\nu \equiv KJ_0$$

$$f(\Delta\nu) = K \int_0^{\infty} \mathcal{E}(\nu - \nu/2) \mathcal{E}(2\nu_0 - \nu + \nu/2) d\nu \equiv KJ(\Delta\nu)$$

where J_0 is the overlap of the absorption and fluorescence, $J(\Delta\nu)$ is the shifted overlap of the absorption and "effective" emission peak, and K contains the remaining terms from Eqns III-27.

The memory function then becomes:

$$\Phi(t) = (\pi J_0)^{-1} \int_{-\infty}^{\infty} J(\Delta\nu) \cos(\Delta\nu t) d\Delta\nu \quad (4)$$

which is like the Fourier transform of the curve representing the overlap integral as a function of the peak shift.

We will now derive specific forms for $\phi(t)$ using Gaussian and Lorentzian line profiles, and assuming mirror image symmetry between absorption and fluorescence.

GAUSSIAN: A Gaussian profile is given by:

$$f(v) = f_m e^{-\frac{1}{2} \beta^2 (v - v_a)^2} \quad (5)$$

The over-lap is then:

$$J_0 = f_m^2 \frac{\sqrt{\pi}}{\beta} e^{-\beta^2 v_s^2 / 4} \quad (6)$$

where: $v_a \equiv$ wave number of the absorption maximum

$v_s \equiv$ stokes shift = $2(v_a - v_0)$

$v_{1/2} \equiv$ half-width-at-half-maximum

$\beta \equiv \sqrt{2 \ln 2} / v_{1/2}$

$J(\Delta v)$ is then easily defined as:

$$J(\Delta v) = f_m^2 \frac{\sqrt{\pi}}{\beta} e^{-\beta^2 (v_s - \Delta v)^2 / 4} \quad (7)$$

The memory function is then given by:

$$\phi(t) = \frac{1}{\pi} \int_{-\infty}^{\infty} e^{-\beta^2 / 4 (\Delta v^2 - 2v_s \Delta v)} \cos(\Delta v t) d\Delta v \quad (8)$$

If we set $\cos(\Delta vt) = \text{Re}(e^{i\Delta vt})$,

then Eqn 8 becomes

$$\phi(t) = \frac{1}{\pi} \text{Re} \int_{-\infty}^{\infty} e^{-\left[\frac{\beta^2}{4} \Delta v^2 - (\frac{\beta^2}{2} v_s + it) \Delta v\right]} d\Delta v \quad (9)$$

using Eqn 7.4.32 from Abrahamowitch and Stegun (1965) and the limit (7.1.29):

$$\lim_{x \rightarrow \infty} (\text{erf}(x+iy)) = 1$$

we can integrate Eqn 9 and obtain:

$$\begin{aligned} \phi(t) &= \frac{2}{\beta \sqrt{\pi}} e^{\left(\frac{\beta^2}{4} v_s^2 - \frac{t^2}{\beta^2}\right)} \cos(v_s t) \\ &= \left[0.96 v_{1/2} e^{0.35 \left(\frac{v_s}{v_{1/2}}\right)^2} \right] e^{-0.721 v_{1/2}^2 t^2} \cos(v_s t) \end{aligned} \quad (10)$$

LORENTZIAN: A Lorentzian profile is given by:

$$E(\nu) = E_m \frac{\nu_{1/2}}{\pi} \frac{1}{(\nu - \nu_a)^2 + \nu_{1/2}^2} \quad (12)$$

The memory function is given by:

$$\phi(t) = \frac{E_m \nu_{1/2}}{\pi^2 J_0} \int_{-\infty}^{\infty} d\Delta \nu \cos(\Delta \nu t) \int_0^{\infty} \frac{1}{(\nu - \nu_a)^2 + \nu_{1/2}^2} \times \frac{1}{[\nu - (\nu_a - \nu_s + \Delta \nu)]^2 + \nu_{1/2}^2} d\nu \quad (13)$$

Using Eqn 3.724.2 from Abrahamowitch and Stegun (1965) we get:

$$\phi(t) = \frac{E_m}{\nu_{1/2} J_0} e^{-2\nu_{1/2} t} \cos(\nu_s t) \quad (14)$$

Normalizing $\phi(t)$ such that $\phi(0) = 1$, we finally obtain:

$$\begin{aligned} \phi_g(t) &= e^{-0.721 v_{1/2}^2 t^2} \cos(v_s t) && \text{:Gaussian} \\ \phi_l(t) &= e^{-2 v_{1/2} t} \cos(v_s t) && \text{:Lorentzian} \end{aligned} \quad (15)$$

An important parameter in $\phi(t)$ is the time constant in the exponential:

$$\begin{aligned} \alpha_g &= 0.85 v_{1/2} && \text{: Gaussian} \\ \alpha_l &= 2.0 v_{1/2} && \text{: Lorentzian} \end{aligned} \quad (16)$$

$\phi(t)$ is plotted in Fig. 9 for chl-a in ether using a value of $v_{1/2} = 188 \text{ cm}^{-1}$, $v_s = 161 \text{ cm}^{-1}$ and the Gaussian and Lorentzian approximation for the main peak at 660 nm.

We see that $\phi(t)$ has dropped about 80% when $t = 1/\alpha$ and is essentially zero by $t \approx 3 \times 10^{-13}$ sec. For a Stokes shift of $v_s = 184 \text{ cm}^{-1}$ the cosine variation is not significant.

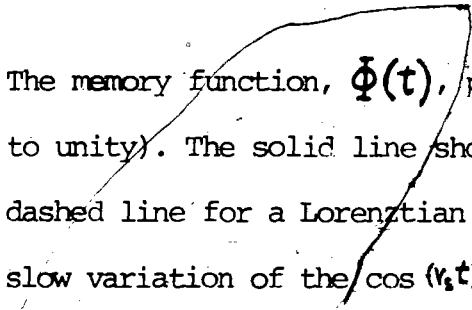
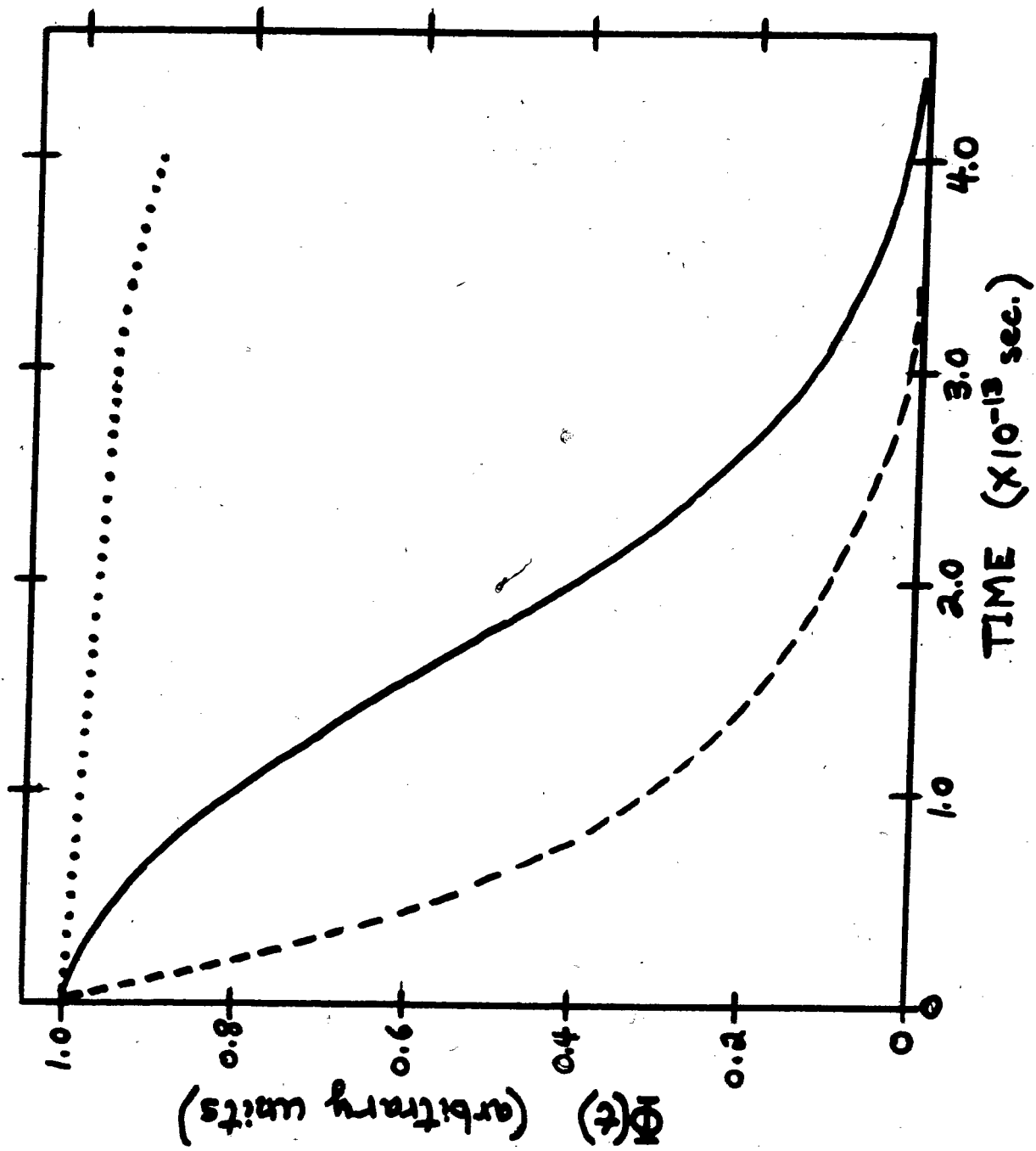
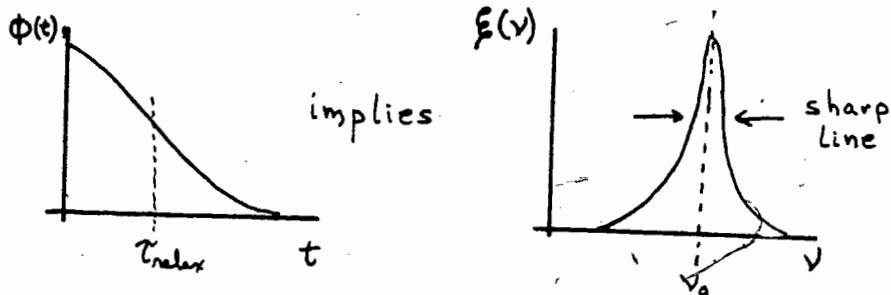


Fig. 9 The memory function, $\Phi(t)$, plotted against time, (normalized to unity). The solid line shows Φ for a Gaussian and the dashed line for a Lorentzian profile. The dotted line shows the slow variation of the $\cos(v_s t)$ factor, neglected in Eqn. 10, compared to the exponential part.



α is a measure of how fast the localization of excitation takes place. For excitation lifetimes greater than $1/\alpha$ the energy transfer process can be considered Markoffian. For times much greater than $1/\alpha$ or for very large α , $\phi(t) \approx \delta(t)$ and the GME reduces to the PME describing a random hopping of excitation as discussed before. Thermal relaxation times have a lower limit estimated to be in the range of about 3×10^{-13} sec. (Dexter and Knox, 1965). We see that $\phi(t)$ has dropped to zero before this, (Fig. 9), indicating that thermal relaxation destroys all phase relationship between the excitation on neighbouring molecules, thus effectively randomizing the transfer process.

If $\phi(t)$ is not zero for times greater than the thermal relaxation time we have a small α and therefore a narrow line width (small $\nu_{1/2}$) (because of the Fourier transform property). i.e.



This is possible for systems that have discrete sharp vibrational bands such as atomic or simple molecules, which means that the vibrational quanta are much greater than the phonon energies, (kT) , or the collisional energy. Thus they do not couple very well to the "thermal bath" and thermal relaxation occurs only very slowly. Therefore it is possible to maintain coherence of the excitons over a longer period of time. "Sharper peaks in the spectra would mean smaller interactions with phonons and the environment and a correspondingly longer memory" (Knox and Kenkre, 1974).

Chlorophyll has a continuous spectrum. Therefore it couples very readily to the environment. This is reflected in its wider band width and sharper memory function.

v) solution of the GME

We have now derived and discussed the memory function $\Phi(t)$ for the GME, (Eqn 2), and will now proceed to solve the GME, by calculating the mean square displacement of excitation and finally obtain an expression relating the transfer rate and interaction energies for Gaussian and Lorentzian line profiles.

In our model we assume the molecules have an average spacing, The mean square displacement of the excitation is:

$$\langle x^2 \rangle = \frac{\sum_m (m^2 a^2) P_m}{\sum_m P_m} = \langle m^2 \rangle a^2 \quad (17)$$

where P_m is the probability that the excitation is on molecule m .

We define the rate of excitation transfer, w , as the inverse of the time required for $\langle x^2 \rangle$ to build up from zero to the value, a^2 . This definition will apply to the full range of intermolecular coupling strengths and is not restricted to pairwise interactions.

Differentiate Eqn 17 and setting $\sum_m P_m = 1$, we find

$$d\langle x^2 \rangle / dt^2 = \sum_m (m^2 a^2) dP_m / dt$$

Substituting the GME:

$$dP_m / dt = \int_0^t ds \phi(t-s) \cdot \sum_n [F_{mn} P_n(s) - F_{nm} P_m(s)]$$

we obtain

$$\frac{d\langle x^2 \rangle}{dt} = a^2 \int_0^t ds \phi(t-s) \sum_m \sum_n m^2 [F_{mn} P_n(s) - F_{nm} P_m(s)]$$

Interchanging dummy subscripts in the second term:

$$\sum_m \sum_n m^2 F_{nm} P_m(s) \longrightarrow \sum_m \sum_n n^2 F_{mn} P_n(s)$$

we obtain

$$d\langle x^2 \rangle dt^2 = a^2 \int_0^t ds \phi(t-s) \sum_m \sum_n F_{mn} (m^2 - n^2) P_n(s)$$

Next we assume that the transfer is homogeneous or isotropic:

$F_{n+x,n} = F_{n-x,n}$. Shifting the "origin" of the "count" such

that: $F_{n+x,n} = F_{n-x,n} = F_l$ where $l = m-n = x$ so that

$$\sum_m F_{mn} (m^2 - n^2) = \sum_l F_l (l^2 + 2nl)$$

Our double sum becomes:

$$\sum_m \sum_n F_{mn} (m^2 - n^2) P_n(s) = \sum_n \left(\sum_l F_l l^2 + 2n \sum_l F_l l \right) P_n$$

We further introduce the assumption that the forward rate equals the backward rate: $F_l = F_{-l}$. Therefore the second term becomes identically zero, leaving:

$$\sum_n \sum_l F_l l^2 P_n(s) = \sum_n \sum_m F_{mn} (m-n)^2 P_n(s)$$

We are finally left with:

$$\overline{d\langle x^2 \rangle / dt^2} = \int_0^t ds \phi(s) \langle A \rangle \quad (18)$$

$$\text{where } \langle A \rangle = \sum_n P_n(s) \cdot \sum_m F_{mn} (m-n)^2 a^2$$

The result has validity in more than one-dimension as can be seen by working through the above derivation making the following changes:

$$\sum_m \rightarrow \sum_{\vec{m}} \quad m \rightarrow \vec{m} \quad m^2 \rightarrow \vec{m} \cdot \vec{m}$$

and similarly for n.

Now according to our definition of transfer rate $w = 1/t$, we can solve for w by integrating Eqn 18

$$\int_0^{1/w} d\langle x^2 \rangle / dt dt = a^2 = \int_0^{1/w} dt \int_0^t ds \phi(s) \langle A \rangle \quad (19)$$

From Appendix C, the time dependent transition rates of the GME, $w_{mn}(t-s)$ have the following form:

$$w_{mn}(t-s) = 2|u|^2 / \hbar^2 \cdot \phi(t-s)$$

where the memory term ϕ is a time decaying oscillatory factor such as Eqn 15 and U is the interaction energy between sites m and n.

We have already chosen to separate out the time dependence in $w_{mn}(t-s)$ and write it as:

$$w_{mn}(t-s) = F_{mn} \phi(t)$$

Therefore we make the following identification:

$$F_{mn} \phi(t) = 2 \frac{|u|^2}{\hbar^2} e^{-\left\{ \begin{array}{l} \alpha_g^2 t^2 \\ \alpha_l t \end{array} \right\}} ; \left\{ \begin{array}{l} \text{Gaussian} \\ \text{Lorentzian} \end{array} \right\} \quad (20)$$

where we have dropped the cosine terms because of their negligible contribution in our case. α_g and α_l are defined as in Eqn 16.

We will now proceed to solve Eqn 19 for Gaussian and Lorentzian profiles for nearest neighbour interaction on a square lattice. In this case let $P_n = 1/4$.

A) GAUSSIAN PROFILE

By summing over the four nearest neighbours:

$$\phi(s) \langle A \rangle = \frac{2|u|^2}{\hbar^2} e^{-\alpha_g^2 t^2} \cdot \frac{1}{4} \cdot 4a^2$$

and substituting in Eqn 19 we get:

$$2 \frac{|u|^2}{\hbar^2} \cdot a^2 \cdot \int_0^{k_w} dt \int_0^t e^{-\alpha_g^2 s^2} ds = a^2$$

which is:

$$\frac{|u|^2}{\hbar^2} \frac{\sqrt{\pi}}{\alpha_g} \int_0^{k_w} \text{erf}(\alpha_g t) dt = 1$$

Using the result for the indefinite integral (Abrahamowitch and Stegun 1965):

$$\int \operatorname{erf}(x) dx = x \operatorname{erf}(x) + \frac{1}{\sqrt{\pi}} e^{-x^2} + \text{const.}$$

we obtain:

$$\sqrt{\pi} \left(\frac{\alpha_g}{w} \right) \operatorname{erf} \left(\frac{\alpha_g}{w} \right) + e^{-\alpha_g^2/w} - 1 = \frac{\alpha_g^2 \hbar^2}{|u|^2} \quad (21)$$

We now have an equation for, w , the nearest neighbour transfer rate in terms of $|u|$, the interaction energy. α_g enters as a parameter and its value is a property of the molecules involved We will apply Eqn 21 to our PSU model with α_g defined for chl-a in ether in the next section. But first let us see whether Eqn 21 gives the correct results in the limits of strong and weak coupling.

a) very-weak coupling limit: $\alpha_g \gg |u|/\hbar$

$$\operatorname{erf}\left(\frac{\alpha}{w}\right) \rightarrow 1 \quad ; \quad e^{-\alpha^2/w^2} \rightarrow 0$$

Eqn 21 becomes:

$$w = \frac{4\pi^{5/2} |u|^2}{\alpha_g \hbar^2} \quad (22)$$

Previously we saw that (Eqn III-26)

$$w = \frac{4\pi^2 |u|^2}{\Delta E \hbar}$$

Comparing this with Eqn 22 we can make the following identification between α and the Franck-Condon band-width, ΔE :

$$\alpha = \frac{\sqrt{\pi}}{\hbar} \Delta E$$

b) strong limit: $\alpha_g \ll \frac{|u|}{\hbar}$

$$\operatorname{erf}\left(\frac{\alpha}{w}\right) \approx \frac{2}{\sqrt{\pi}} \frac{\alpha}{w} \quad ; \quad e^{-\alpha^2/w^2} \approx 1 - \frac{\alpha^2}{w^2}$$

Eqn 21 becomes

$$w = 2\pi \frac{|u|}{\hbar} \approx 4 \frac{|u|}{\hbar}$$

Which is what we obtained in Eqn III-21. Eqn 21 gives the correct results in the "fast" and "slow" limits of energy transfer and provides a connecting formula for the intermediate region.

II) LORENTZIAN PROFILE

We have as before:

$$\phi(s) \langle A \rangle = 2 \frac{|u|^2}{\hbar^2} e^{-\alpha_e t} \cdot \frac{1}{4} \cdot 4a^2$$

substituting into Eqn 19 gives

$$2 \frac{|u|^2}{\hbar^2} \int_0^{1/w} dt \int_0^t e^{-\alpha_e s} ds = 1$$

Integration gives:

$$\frac{\alpha_e}{w} + e^{-\alpha_e/w} - 1 = \frac{\hbar^2 \alpha_e^2}{2 |u|^2} \quad (23)$$

In the very-weak limit we get: $(\alpha \gg |u|/\hbar)$

$$w = \frac{8\pi^2 |u|^2}{\hbar^2 \alpha}$$

with

$$\Delta E = \frac{\hbar}{2} \alpha$$

In the strong limit we get: $(\alpha \ll |u|/\hbar)$

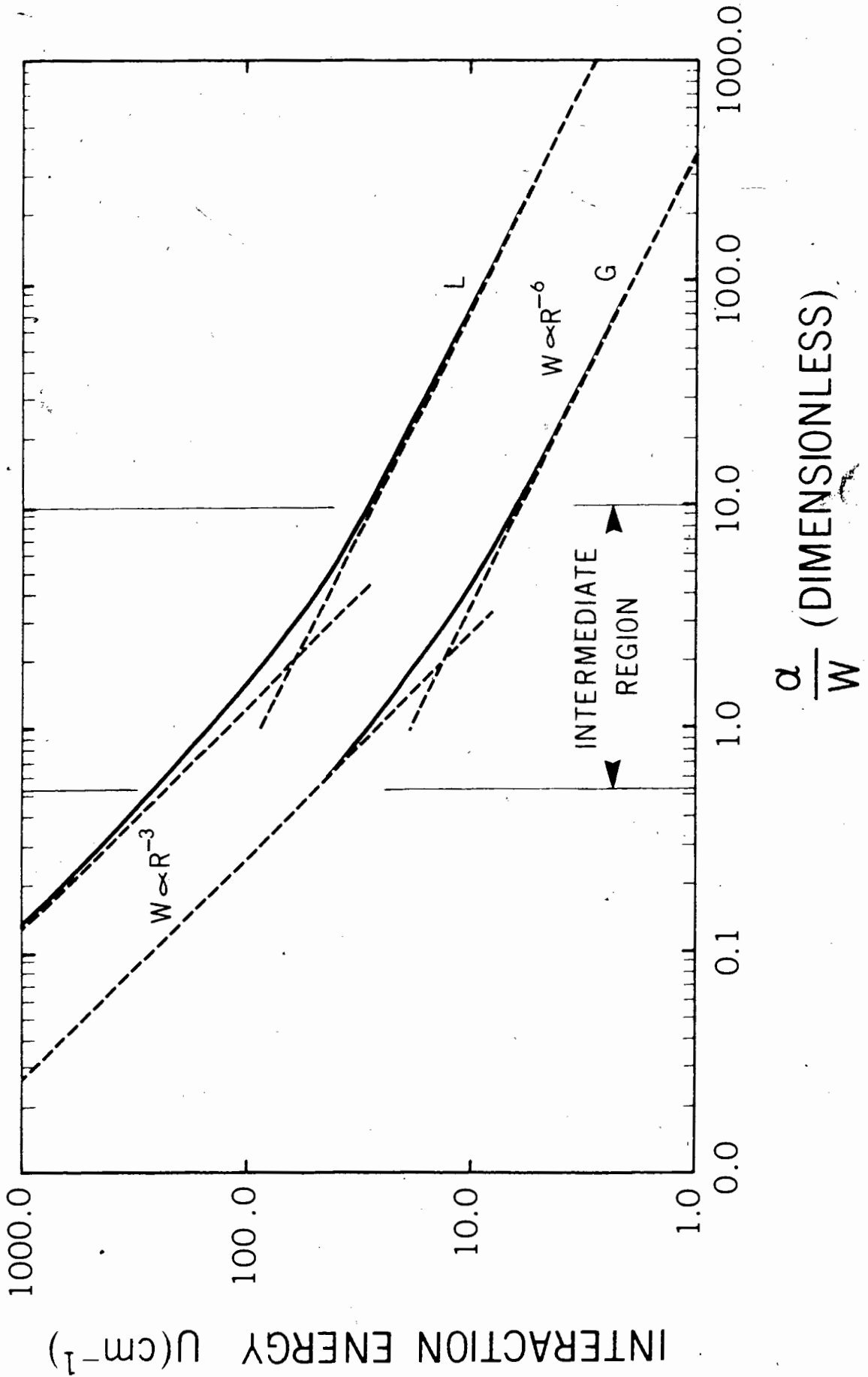
$$w = \frac{2\pi |u|}{\hbar}$$

The limits are calculated in the same manner as for Eqn 21. Eqns 21 and 23 are plotted in Fig. 10 as interaction energy against $\frac{\omega}{w}$. We can see the continuous change from very-weak to strong coupling. The asymptotic limits of strong and very-weak coupling are represented by dotted lines, and the intermediate region of weak coupling is illustrated. Note that it is not enough to specify w in order to say which of the three mechanisms is in effect. The ratio $\frac{\omega}{w}$ determines this. Energy transfer is fast or slow relative to α .

We have not specified what form the interaction energy will take, whether dipolar, quadrupole, etc. We have seen that if the interaction is point dipole-dipole then the transfer rate varies as R^{-3} for the strong coupling case, and as R^{-6} for the very weak case. We will now show that these results are also obtained from the GME solutions (Eqns 21 and 23) in the two limits. Furthermore we will be able to determine the exponent, N , in the relation $w \propto R^{-N}$ for intermediate cases.

Fig. 10 The solution of the generalized master equation for Gaussian, G, and Lorentzian, L, absorption profiles, corresponding to Eqns IV-21 and IV-23. The dotted lines are the asymptotes for the limits of strong and very-weak coupling.

ms. work on original



original

First we assume that the interaction energy is dipole-dipole.

$$|u| \propto R^{-3}$$

and express the transfer rate as:

$$w \propto R^{-N} \tag{24}$$

The exponent can be expressed as:

$$N = - \frac{d \ln w}{d \ln R}$$

By taking the logarithm of Eqn 21 and differentiating with respect to $\ln R$ we obtain for Gaussian profile

$$N = 6 \cdot \left[1 + \frac{e^{-d^2/w^2} - 1}{\sqrt{\pi} \left(\frac{d}{w}\right) \operatorname{erf}\left(\frac{d}{w}\right)} \right] \tag{25}$$

and similarly from Eqn 23 for Lorentzian profile

$$N = 6 \cdot \left[\frac{1}{(1 - e^{-d/w})} - \frac{w}{d} \right] \tag{26}$$

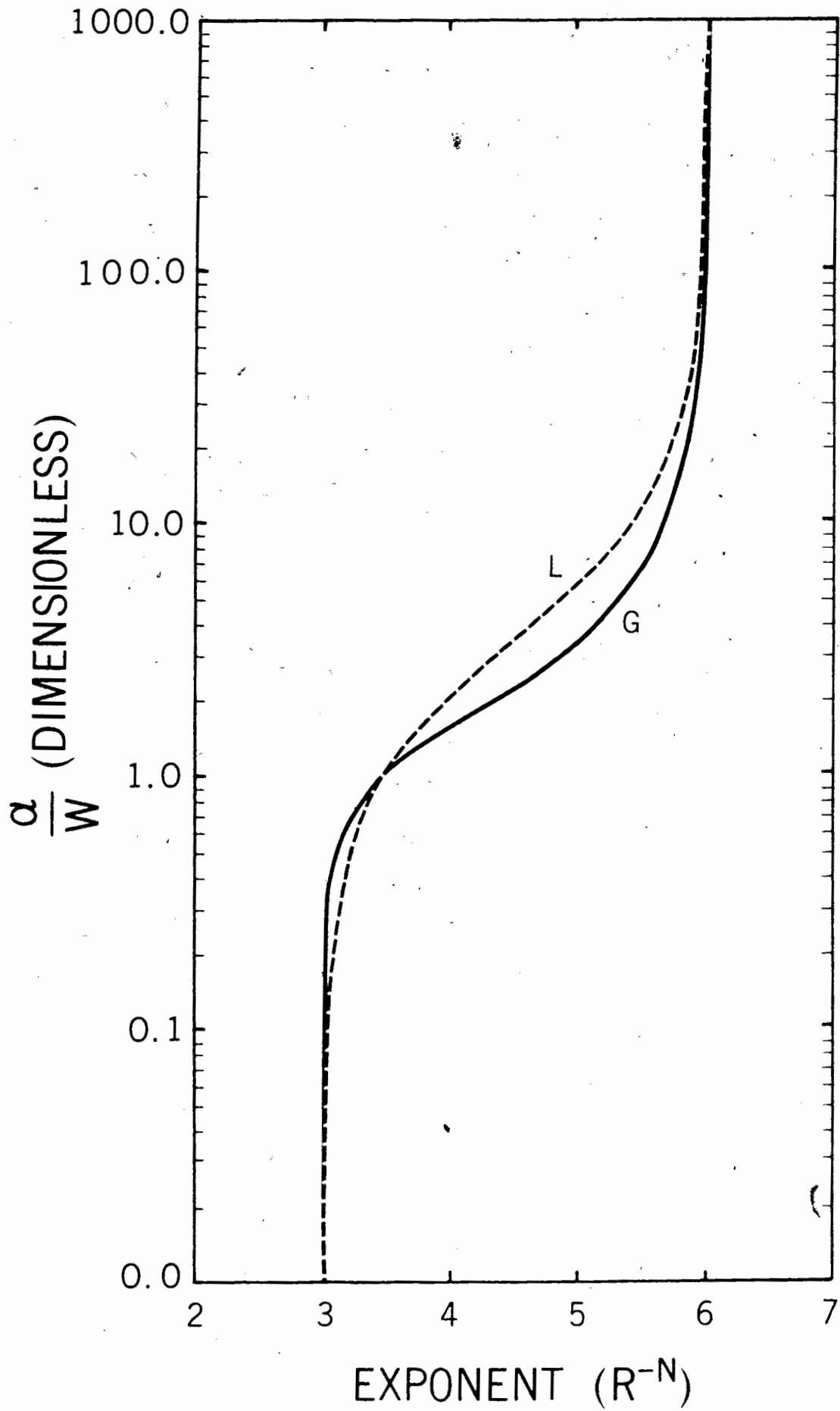
The limiting behaviour for Eqns 25 and 26 is as follows:

$$\lim_{\alpha/w \rightarrow \infty} n = 6 \quad \text{:very-weak coupling}$$

$$\lim_{\alpha/w \rightarrow 0} n = 3 \quad \text{:strong coupling}$$

The results agree with earlier derivations presented in Section III. The exponent n as a function of α/w is plotted in Fig. 11.

Fig. 11 The R^{-N} variation of the transfer rate as a function of ω/ω_r , given by the GME theory, Eqns IV-25 and IV-26 assuming a dipole-dipole interaction for Gaussian, G, and Lorentzian, L, absorption profiles.



vi) summary

We have presented a method for calculating transfer rate in terms of intermolecular interaction energy by solving a generalized master equation for energy transport based on the work of Knox and Kenkre (1974). We have seen that it agrees with previous formulations of the energy transfer problem in molecular systems such as the Forster theory. Its value lies in the fact that it connects strong and very-weak coupling limits allowing one to estimate the extent of the weak coupling region and the transfer rate in this region.

One begins by calculating the memory function from Eqn 4 using the monomer spectrum of the molecule in question. From this one extracts the parameter α . Eqn 18 can then be solved for the desired relation between transfer rate and interaction energy. This has been done for Gaussian and Lorentzian profiles and the results are given by Eqns 21 and 23.

The definition of transfer rate should be kept in mind. It is the reciprocal of the time required for the RMS displacement of the excitation to reach a value, a , which we have chosen to be the mean spacing between neighbouring molecules. Whether energy transport proceeds by diffusion or excitons depends on the value a/w not just on w itself. If the transfer rate falls in the region of very weak coupling, the energy transfer can be described by the Förster theory. In the strong coupling region, w describes the velocity of an exciton which is a/w . Thus our definition of transfer rate is general and is a smooth continuous function of the interaction energy, (Eqns 21 and 23).

V. APPLICATION TO THE PSU

i) "in vitro" absorption spectrum of chl-a and its memory function

We will now apply our results to the model of the PSU described in Section II.

First we must determine the parameter α , from the monomer spectrum of chl-a.

Fig. 12 shows the absorption spectrum of a dilute solution of chl-a in ether. The interpretation of the spectrum is summarized as follows: (Clayton, 65; Sauer, 1970). The main absorption bands are the Soret band around 400 nm and the long-wave band around 600 nm. These bands are the result of singlet electronic transitions of the delocalized electrons around the porphyrin ring. Studies of dichroism have shown that the dipole moments of these transitions lie in the plane of the porphyrin ring of the chl-a molecule. The hydrocarbon phytol chain does not appreciably affect either the band shape or the position of the absorption bands (Goedheer, 1966). In the π^* transition the orbital angular momentum of the singlet excited state can be parallel or antiparallel to the ground state. The former results in the long-wave band, the latter in the Soret band.

The long-wave band is the one responsible for energy transfer among chl-a antennae to the reaction center. The Soret band is not directly involved in this process. Energy absorbed in the Soret band is rapidly degraded by intermolecular vibrations and transferred to the red band. No fluorescence can be observed corresponding to the Soret band. We will only consider the long-wave band from now on.

The main transition is at 660 nm with a vibrational satellite at 613 nm. The transition moments for these are oriented in the direction indicated by the y-axis in Fig. 5. They are referred to in the literature as $Q_y(0 \leftarrow 0)$ and $Q_y(1 \leftarrow 0)$. The very weak peaks at 575 nm and 530 nm are also the result of singlet π^* transitions with spin parallel to the ground state, but having the transition moments oriented perpendicular to the Q_y bands along the shorter axis indicated as x in Fig. 5. We will neglect these two as their contribution is not significant for our considerations.

In Fig. 13 we have enlarged the $Q_y(0 \leftarrow 0)$ and $Q_y(1 \leftarrow 0)$ bands and fitted them with Gaussian and Lorentzian profiles. It is readily apparent that the 660 nm band, $Q_y(0 \leftarrow 0)$ is very nearly Gaussian in shape. The 613 nm band, $Q_y(1 \leftarrow 0)$ is difficult to fit because of its small size, so we have assumed it to be Gaussian also. The fluorescence spectra is very nearly a mirror image of the 660 and 613 nm bands. (Goedheer, 1966). The emission maximum is located at

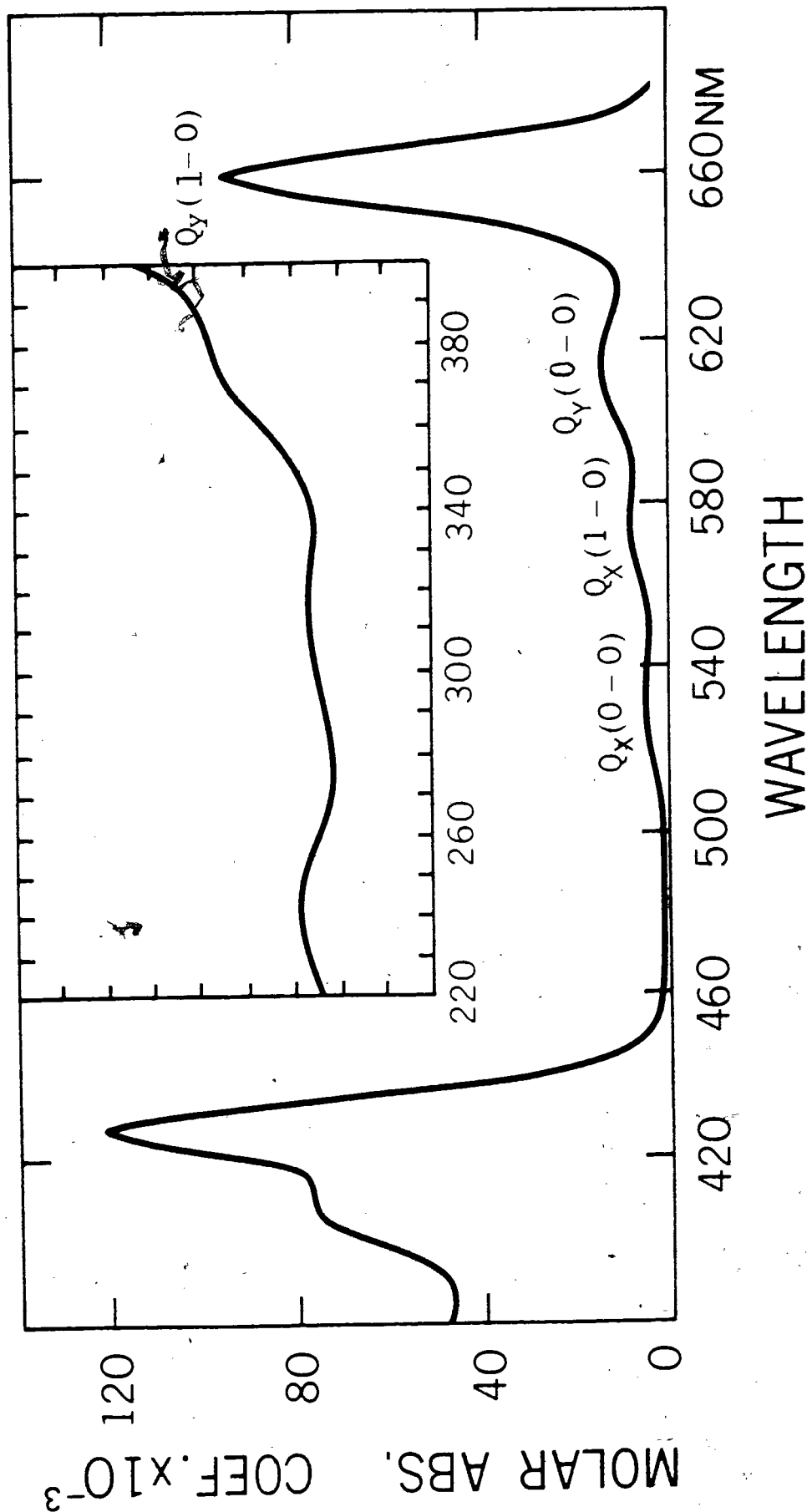
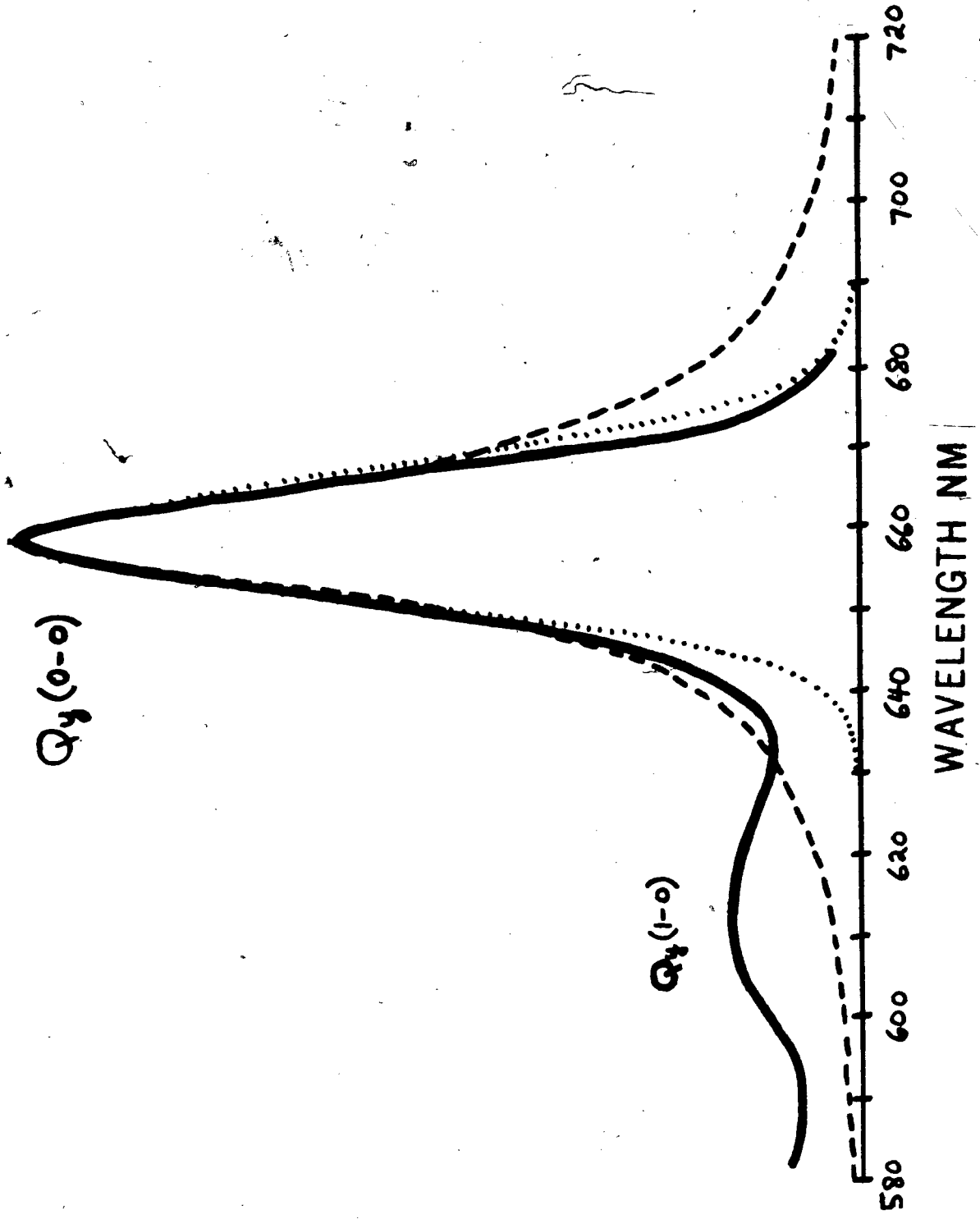


Fig. 12 Absorption spectrum of chl-a in ether. Adapted from C.S. French (1960)

Fig. 13 Gaussian (.....) and Lorentzian (-----)
line profiles fitted to the red absorption band of
chl-a in ether. (Data is from Fig. 12)



668nm, and the Stokes shift is 161cm⁻¹. This adds further weight to the interpretation of the 613 nm band as a vibrational satellite to the 660 nm absorption band. Our assumption of mirror-image fluorescence in deriving our relationships for the memory function $\phi(t)$ and α is therefore satisfied.

For a single component (single Gaussian or Lorentzian) Eqn IV-16 gives α immediately. The half-width of the 660 nm band is 188 cm⁻¹. Therefore:

$$\alpha_g = (0.85) \times (188) \times (3 \times 10^{10}) = 4.794 \times 10^{12} \text{sec}^{-1}$$

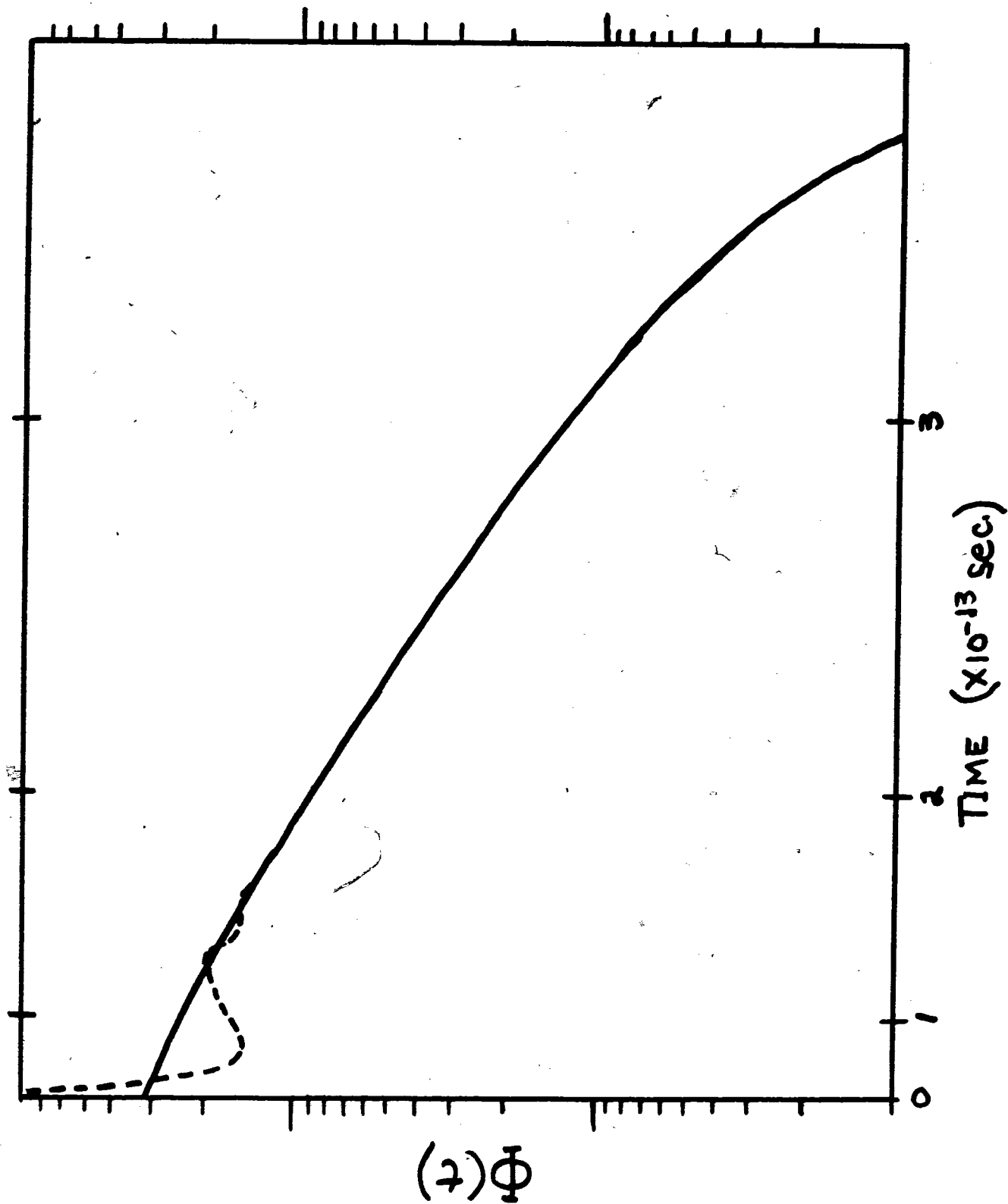
.....Gaussian

$$\alpha_l = (2.0) \times (188) \times (3 \times 10^{10}) = 1.128 \times 10^{13} \text{sec}^{-1}$$

.....Lorentzian

If we include the 613 nm satellite then we must rework Eqn IV-4 for two components. This we have done numerically and the results are shown in Fig. 14 for the spectrum shown in Fig. 13 fitted with two Gaussians. $\phi(t)$ for a single Gaussian, solid line, is shown for comparison. $\phi(t)$ for the double Gaussian, dotted line, falls quickly into line with the single component. The satellite does very little to change $\phi(t)$ other than for a small oscillation at the beginning. This would not change the value of α obtained from the slope of Fig. 14, significantly from the single Gaussian value. Therefore we will use the above values for computed from Eqn IV-16.

Fig. 14. Comparison of the memory function Φ for single component (660 nm) and double component Gaussian absorption band (660 nm and 613 nm). Data is from Fig. 12. Numerically calculated from Equation IV-2.

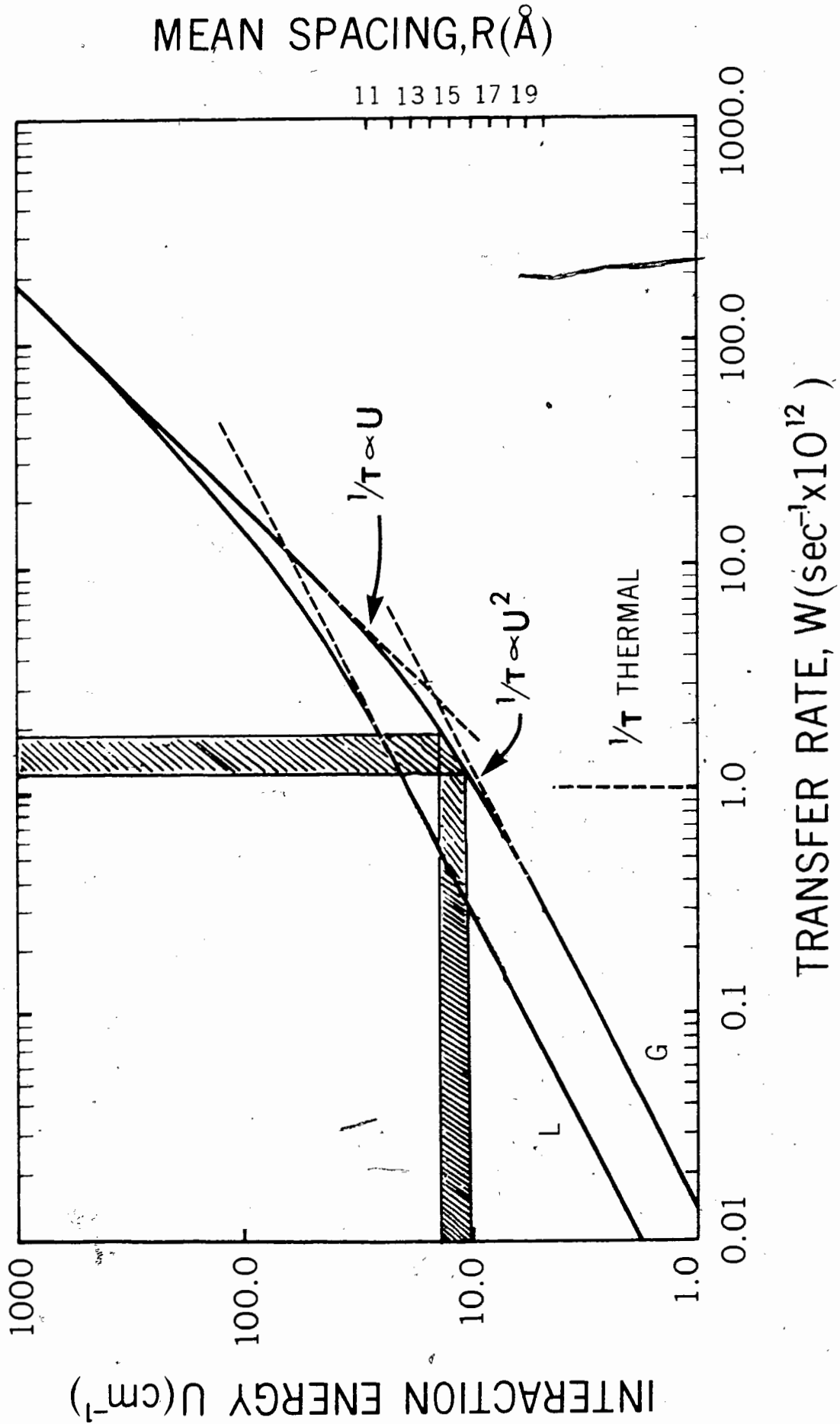


Knowing α we can now determine transfer rate (w) as a function of interaction energy (u) from Eqn IV-21 for Gaussian profiles. This function is plotted in Fig. 15. The result for a Lorentzian with the same half-width is also plotted from Eqn IV-23 for comparison. The curve clearly illustrates the extent to which the transfer rate is the result of very-weak coupling given by Eqn III-26 and the strong coupling, Eqn III-21 and connection between the two in the intermediate or weak coupling region. The asymptotes for the limits of strong and very-weak coupling given by Eqns III-21 and III-26, which have been shown to be the appropriate limits of Eqns IV-21 and IV-23, are also plotted.

A characteristic of the Lorentzian profile is the larger extent of the weak-coupling for larger interaction energies. Weak coupling for Gaussian quickly falls in line with the fast transfer rate asymptote. For dipole-dipole interaction the limits are $w \propto R^{-3}$ and R^{-6} as given by Eqns. IV-25 and IV-26.

Thus knowing the spectral properties of chl-a, Eqn IV-21 describes the excitation transport of an array of chl-a molecules in a thermal bath.

Fig. 15 Transfer rate vs. interaction energy as predicted by the GME solution, Eqn IV-21, for the 660nm band of chl-a fitted with a Gaussian profile, G. ($\alpha_g = 4.8 \times 10^{12} \text{ sec.}^{-1}$) Curve L is a Lorentzian fit, Eqn IV-23 for comparison. ($\alpha_l = 1.13 \times 10^{13} \text{ sec.}^{-1}$) Shaded region indicates the range of transfer rates deduced from the experimental fluorescence lifetimes. Mean-spacing values are from Fig. 16 and correspond to the chl-a separation needed to produce the interaction energies on the left-hand axis assuming a dipole-dipole approximation and the dipole orientation of 35° with the plane used in this model.



ii) application of the GME to the PSU model

Experimentally we are given the fluorescence lifetime which as we have shown is also the mean trapping time τ_t (Section II). If our energy transfer process is Markoffian, indicated by the fact that $\phi(t)$ would be very small for t approximately equal to $1/w$, then the excitation hops from site to site and τ_t is given by:

$$\tau_t = \langle n \rangle 1/w = \langle n \rangle \tau_j \quad (1)$$

where $\langle n \rangle$ is the average number of steps taken to reach the trap and τ_j is the nearest neighbour transfer time equal to $1/w$ the reciprocal of the transfer rate.

Montroll (1969) has worked out an asymptotic expression for the random walk on a lattice with one trap giving the average number of steps. The result for two dimensions is:

$$\langle n \rangle = N \ln N / \pi + 0.195056N - 0.1170 + \Theta(N^{-1}) \quad (2)$$

where N is the number of lattice points, in this case antenna chlorophyll.

The relationship given by Eqns 1 and 2 is only valid if $\alpha/w > 10$ as shown in Fig. 15. However we expect that three factors would destroy the coherent nature of exciton transport and lead to a diffusion of energy rather than wave-like propagation as discussed in Section III. These factors are:

- 1) chlorophyll molecules are not regularly spaced but randomly spaced with a mean spacing of $15 \pm 1 \text{ \AA}$
- 2) their orientation is likely to vary somewhat from that given in Section II.
- 3) chlorophyll molecules are polyatomic and therefore having a high density of vibrational states, lend themselves to a high degree of exciton-phonon scattering when immersed in the "lipid-thermal bath".

The effect of randomness in spacing and orientation on the scattering of excitons was investigated by K. Katasura (1964). For a one dimensional lattice of dipoles with strong coupling, he calculated the time dependence of the RMS displacement of excitation for varying degrees of variance in the lattice spacing and orientation of the dipoles. He found that the RMS displacement of excitation soon becomes dependent on the square root of time as required for diffusion (Section III).

In the weak coupling region the coherent propagation is even more sensitive to disruption (Forster, 1967; Section III). We therefore assume the validity of the random walk equation for our model

Fluorescence lifetimes (trapping times) for P.S. II of plants and algae are typically (See Section II)

0.4 + 0.1 nsec.

for low light levels implying that the traps are open for excitation (Muller, Lumry, walker, 1969).

The number of antenna chlorophyll in P.S. II range from about (Section II)

250 to 350

With these values, the average number of transfers needed to reach the trap is by Eqn 2

488 to 721

This then gives by Eqn 1 the range of transfer rates (inverse transfer time):

$$w = (1.2 \text{ to } 1.8) \times 10^{12} + 0.1 \text{ sec}^{-1}$$

This range of w corresponds to a range of interaction energy predicted by the GME theory from Eqn IV-21 or Fig. 15 as:

$$u = 10 \text{ to } 13 \text{ cm}^{-1}$$

The lower value corresponds to the assumption of 250 antenna chlorophyll, the upper value to 350

Now we will calculate $|u|$ independently from the model assumptions of mean spacing, orientation, and the chl-a absorption spectrum.

Let us suppose that the interaction is entirely dipole-dipole in nature. Then the interaction energy is given by: (Jackson, 1962; Forster, 1965)

$$u = \frac{1}{h^2 |R_{ab}|^3} \left\{ (\bar{m}_a \cdot \bar{m}_b) - 3 (\bar{m}_a \cdot \hat{n}) (\bar{m}_b \cdot \hat{n}) \right\} \dots (3)$$

where: n is the refractive index

\vec{m}_a, \vec{m}_b are the transition dipole moments of molecules a and b (esu)

\vec{R}_{ab} is the vector joining the dipoles in (cm)

$\hat{n} \equiv \vec{R}/|R|$ is the unit vector along \vec{R}_{ab}

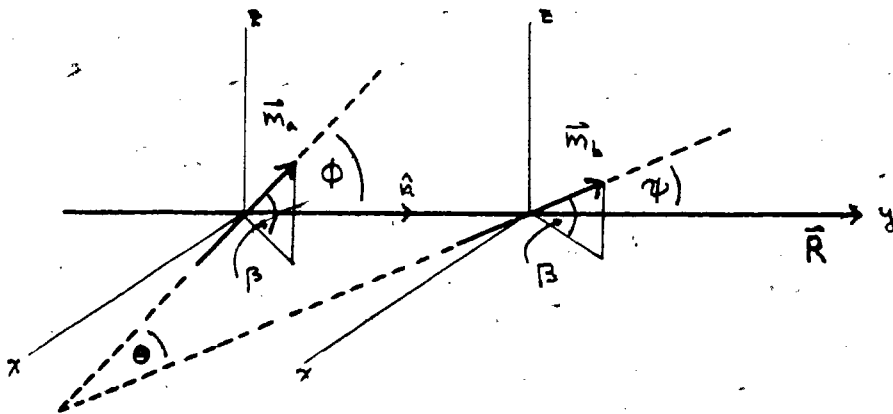
U is the interaction energy in (cm^{-1})

If we take $|\vec{m}_a| = |\vec{m}_b|$ and expand the dot products we get:

$$u = \frac{|M|^2}{n^2 |R|^3} k \quad (4)$$

where $k = \cos \Theta - 3 \cos \phi \cos \psi$

Θ is the angle between the dipoles and ϕ, ψ are the angles the dipoles make with the line joining them as follows:



If the transition moments are allowed to rotate azimuthally maintaining an angle β with the plane of the membrane, then the RMS average of K is (Appendix D):

$$\langle k^2 \rangle = \sin^4 \beta + 5/4 \cos^4 \beta$$

The transition dipole moment is readily obtained from the absorption spectrum (Murrell, 1963):

$$(8\pi^2 mc^3 / 3he^2) |M|^2 = 4.319 \times 10^{-9} \int \epsilon(\nu) d\nu$$

where: ν : wavenumber (cm^{-1})

$\epsilon(\nu)$: extinction coefficient ($\text{cm}^{-1} \text{moles}^{-1} \text{litre}$)

m : electron mass

e : electron charge

c : speed of light

$|M|^2$: dipole moment (esu)

h : Planck's constant

From this we obtain:

$$|M|^2 = 9.184 \times 10^{-39} \left(\int \epsilon(\nu) d\nu / \nu_a \right)$$

where ν_a : absorption maximum

For a Gaussian line shape this becomes (Eqn IV-5)

$$|M|^2 = (1.955 \times 10^{-38}) \epsilon_m (v_{1/2}/v_a)$$

where: $v_{1/2}$: half-width (cm^{-1}) at half maximum

v_a : absorption maximum (cm^{-1})

ϵ_m : extinction coefficient at maximum ($\text{cm}^{-1}\text{moles}^{-1}\text{litre}$)

For chl-a in ether we know the following (Colbow, 1973)

$$\epsilon_m = 85100 \text{ (cm}^{-1}\text{moles}^{-1}\text{litre)}$$

$$v_{1/2} = 188 \text{ (cm}^{-1}\text{)}$$

$$v_a = 15149 \text{ (cm}^{-1}\text{)}$$

Therefore: $|M|^2 = 2.07 \times 10^{-35} \text{ esu}$

The index of refraction n as discussed in Section II is 1.45. The orientation of the transition moment β will be taken to be $35^\circ \pm 2^\circ$ as discussed in Section II. The RMS value of K averaged over all possible azimuthal directions is then from Eqn 5:

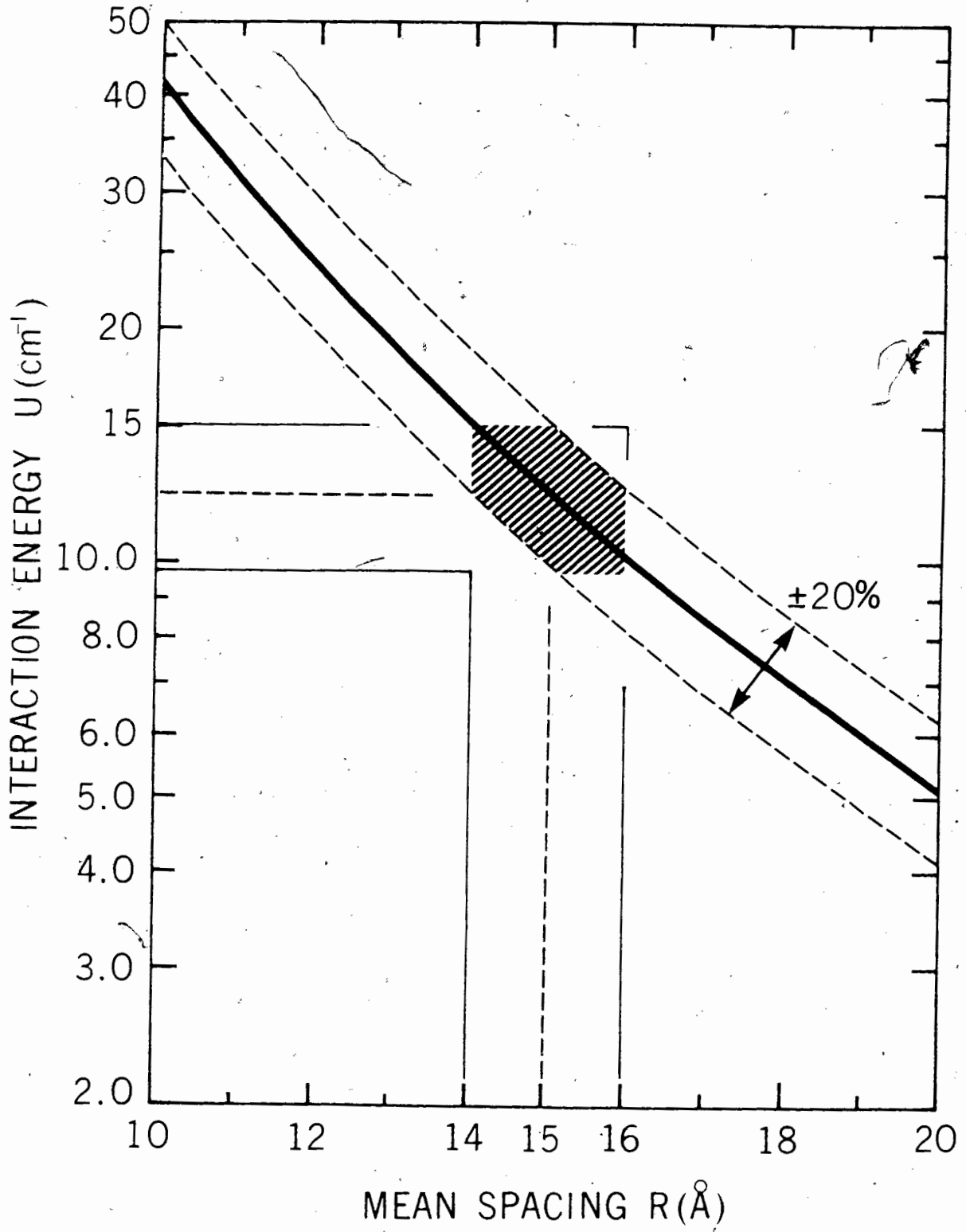
$$\begin{aligned} \langle K^2 \rangle &= \sin^4(35 \pm 2) + 5/4 \cos^4(35 \pm 2) \\ &= 0.82 \pm .02 \end{aligned}$$

We shall now calculate $|u|$ from Eqn 4 for a range of R from 14 to 16 Å, the assumed mean spacing of chl-a in PSII from Section II. This value will then be compared with that calculated previously from Eqn IV-21.

We can make some estimate of the error involved in using the dipole-dipole approximation. Chang (1972) has worked out a correction to the dipole-dipole approximation based on an exact calculation of the transition monopoles. This involves attempting to calculate the orbital wavefunctions. In the range of 15 ± 1 Å the ratio of exact interaction to dipole-dipole calculation for chl-a ranges from 0.7 to 1.4 depending on the orientation. This means that $|u|$ calculated from Eqn 4 may differ by $\pm 20\%$. Eqn 4 is plotted in Fig. 16 for a range of R from 10 to 20 Å and a K value of 0.82. The $\pm 20\%$ possible variation is indicated. The range of $|u|$ corresponding to 15 ± 1 Å predicted by Eqn 4 and Chang's results is about

$$u = 10 \text{ to } 15 \text{ cm}^{-1}$$

Fig. 16 Energy .vs. chl-a separation for dipole-dipole interaction given by Eqn. V-4. The possible $\pm 20\%$ correction for the exact monopole calculation is indicated.



Using this calculated interaction energy of 10 to 15 cm^{-1} , we can substitute into the GME solution, Eqn IV-21 to obtain the nearest neighbour transfer rate (w). The answer is obtained directly from Eqn IV-21 or Fig. 15 as:

$$(1.1 \text{ to } 2.1) \times 10^{12} \text{ sec}^{-1}$$

We can then compare this to the pair-wise transfer rate predicted by the Förster Theory, Eqn III-28, for the same range of interaction energy. Colbow (1973a) determined the transfer rate between chl-a antenna from the Förster Equation using the same mean-spacing and orientation assumptions as in our model and a new value for R_0 of 65.1 Å based on spectroscopic measurements of chl-a in lipid vesicles. (Colbow, 1973b). The rates obtained were:

$$(0.24 \text{ to } 0.64) \times 10^{12} \text{ sec}^{-1}$$

This range is close, but as expected somewhat lower than the predictions of the GME theory as the rates from the Förster Theory fall in the very-weak coupling region but near the intermediate region where the R^{-6} rate dependence applies as indicated in Fig. 15.

The GME theory gives better agreement with experimental data. It also provides an expression useful for calculating transfer rates over a wide range of interaction strengths.

The results are summarized in the accompanying table.

<p>mean spacing of chl-a antenna deduced from experimental measurements on the available area per chl-a molecule of 200\AA^2 to 250\AA^2 (Wolken et. al. 1953; Kreutz, 1970)</p>	<p>calculated interaction energy, (u), Eqn V-4, using experimental measurements of mean spacing and orientation for the chl-a molecules</p> $u = \frac{ \vec{m} ^2}{r^2 R^3} k$	<p>nearest neighbour transfer rate (w) predicted by the Förster theory, Eqn III-28, for the calculated interaction energy and a value of $R_0 = 65.1\text{\AA}$</p> $w = \frac{1}{\tau_0} \left(\frac{R_0}{R} \right)^6$ <p>R_0 includes the fluorescence-absorption overlap</p>	<p>nearest neighbour transfer rate (w) predicted by the solution to the GME Eqn IV-21, for the calculated interaction energy and a value of $\tau_{11} = 4.8 \times 10^{-12}$ sec from the chl-a half-width of the red absorption band</p> $-R \left(\frac{\alpha_2}{w} \right) \exp \left(\frac{\alpha_2}{w} \right) + e^{-\frac{\alpha_2}{w}}$ $-1 = \frac{\alpha_2^2}{w^2}$	<p>nearest neighbour transfer rate (w) deduced from experimental fluorescence lifetimes using the random walk assumption and a range of 250 to 350 antenna chl-a</p> $w = \frac{\langle n \rangle}{\tau_f}$ <p>$\langle n \rangle$: number of steps τ_f : lifetime</p>
<p>14 to 16 A</p>	<p>10 to 15 cm^{-1}</p>	<p>(0.24 to 0.64) $\times 10^{12}$ sec^{-1}</p>	<p>(1.1 to 2.1) $\times 10^{12}$ sec^{-1}</p>	<p>(1.2 to 1.8) $\times 10^{12}$ sec^{-1}</p>

Comparison of the nearest neighbour transfer rates, deduced from experimental measurement, with those predicted by the Förster and GME theories based on the same interaction energy calculated from chl-a spacing and orientation.

iii) the "in vivo" absorption spectrum

The value of the interaction energy, $12 \pm 3 \text{ cm}^{-1}$, predicted by our model, disallows strong exciton splitting of the absorption band "in vivo". The red absorption band of chl-a "in vivo" may be separated into at least three bands with maxima at 673, 683 and 695 nm (Rabinovitch and Govindjee, 1969; Clayton, 1965; Kreutz, 1970). There is strong evidence that this multiplicity of peaks is due to chlorophyll aggregation, rather than interactions with lipids or proteins (Rabinowitch and Govindjee, 1969; Kreutz, 1970; Katz, 1973). There is general agreement that the 683 nm band is due to a dimer (Kreutz, 1970; Clayton, 1965) and the 695 nm band to a stacked chlorophyll polymer (Kreutz, 1970; Katz, 1973; McRae and Kasha, 1964). Whether the 673 nm band is due to a different chlorophyll dimer or represents a monomer is an important unresolved question (Colbow, 1973a). If we consider the 673 nm band as a monomer, then in order to produce the shifts to 683 and 695 nm, interaction energies of 218 and 470 cm^{-1} are required respectively. This would certainly be in the range of strong coupling and would correspond to transfer rates estimated by Eqn. III-15 of 2.6×10^{13} to $5.6 \times 10^{13} \text{ sec}^{-1}$. To account for the observed fluorescence lifetimes, the trapping rate or trapping efficiency would have to be much smaller than the inter-antenna transfer rate in order that the excitation could reside among the antenna long enough to fluoresce with the measured efficiency of 3%. This assumes that single chlorophyll molecules

are arranged uniformly in the PSU all having a sufficiently small spacing required for the interaction energy to be greater than 100 cm^{-1} .

Robinson (1966) discusses such a model where single antenna chlorophyll are arranged uniformly with a mean spacing of 11\AA . The interaction energy is of the order of 100 cm^{-1} , and trapping is the rate determining step.

In this case the excitation soon reaches an equilibrium distribution, where the probability of locating the excitation on any one of the N sites of the PSU is $1/N$ (see Section III). This is directly opposed to the trapping mechanism we have employed in our model described in Section II. Here the rate of trapping is as fast or faster than the inter-antenna transfer rate and proceeds with almost 100% efficiency. Therefore the inter-antenna transfer is the rate determining step. Robinson's model is unacceptable as it is unlikely that all the antennae are close packed with a spacing of 11\AA . This figure is based on the volume of the quantasome. Quantasomes are morphological units observed in chloroplast preparations under the electron microscope and were thought to be photosynthetic units. However they are now considered to be artifacts. (Branton, 1968)

This page is blank. Text is continued
on page 91.

A suggestion (Colbow, 1973) that incorporates both exciton splitting and a low interaction energy (slow transfer rate) between antenna molecules is to locate a chl-a dimer at each antenna site. (two molecules per unit cell). For a PSU of 300 chlorophyll, this would imply a spacing of 23.5 Å. The interaction energy between sites could then be low enough, ($\approx 10 \text{ cm}^{-1}$), to give a slow transfer rate and the strong coupling within the dimer would produce the exciton splitting. In order to treat this variation of the model properly, the intensity, width, and Stokes shift of the red absorption band of the dimer would have to be known. Colbow (1973a) using the Forster theory obtained a value of 9 ns for the mean trapping time in an array of 150 dimers, which is too large by a factor of 10. One of the reasons may be that the natural lifetime τ_0 of chl-a monomers, (15.2 ns), was used in the Forster equation, Eqn. III-19. The natural lifetime of the dimer is probably smaller and could be obtained from the absorption spectrum parameters, if they were known. Also dimers would not probably be as free to rotate azimuthally as single chl-a antenna, so the orientation factor k would be different.

iv) conclusion

For the PSU's of green plants and algae, for which our model is intended, it appears that energy is transferred among the antenna chlorophyll by "vibronic excitons" resulting from the "weak coupling" interaction between the vibrational levels of neighbouring chlorophyll molecules. The wave-like character of the excitons is rapidly destroyed by the variation of spacing and orientation of the molecules in the lipid environment. This means that the excitation motion is not described by a single wave-vector (directionality or coherence). Rather it moves by diffusion, with a speed faster than the diffusion of excitation in the very weak coupling case.

We have also derived an expression, Eqn IV-21, from GME theory relating interaction energy and transfer rate between antenna molecules that gives results in good agreement with experiment. It is also useful over a wide range of interaction strengths.

BIBLIOGRAPHY

- Abrahamovitz, M. and Stegun, I.A. (eds) (1965) Handbook of
Mathematical Functions, Dover, New York
- Bay, Z. and Pearlstein, R.M. (1963a) Proc. Nat. Acad. Sci. 50, 962-967
(1963b) Proc. Nat. Acad. Sci. 50, 1071-1078
- Branton, D. (1968) in Photophysiology pp.197-224
(Giese, A. ed.) Academic Press, New York
- Borisov, A. Yu, and Il'ina, M.D. (1973) Biochim. Biophys. Acta 305,
364-371
- Borisov, A. Yu and Godik, V.I. (1973) Biochim. Biophys. Acta 301,
227-248
- Chang, J.C. (1972) Phd. Thesis. Univ. of Rochester, New York
- Cherry, R.J., Hsu, K., and Chapman, D. (1972) Biochim. Biophys. Acta
267, 512-522
- Clayton, R.K. (1965) Molecular Physics in Photosynthesis, Blaisdel,
New York
- (1971) Light and Living Matter, Vol. 2: The Biological Part,
McGraw-Hill, New York
- (1972) Proc. Nat. Acad. Sci., U.S.A. 69, 44-49
- Colbow, K. (1973a) Biochim. Biophys. Acta. 314, 320-327
(1973b) Biochim. Biophys. Acta. 318, 4-9
- Dexter, D.L. (1953) J. Chem. Phys. 21, 836-850
- Dexter, D.L. and Knox, R.S. (1965) Excitons, Interscience, New York
- Forster, Th. (1967) Comprehensive Biochemistry, 22, 61-80
(1965) in Modern Quantum Chemistry. (O. Sinangulu, ed.)
Vol. III, 93-137, Academic Press, New York
- Franck, J. and Teller, E. (1938) J. Chem. Phys. 6, 861-872
- French, C.S. (1960) in Handbuch der Pflanzenphysiologie Vol. V
no. 1, pp. 252-297, (Ruhland, W. ed.)
Springer-Verlag, Berlin

Goedheer, J.C. (1966) in *The Chlorophylls* (Vernon and Seely, eds) pp 147-184, Academic Press, New York

(1972) *Ann. Rev. Plant Physiol.* 23, 87-112

Govindjee (1974) *Sci. Am.* 231, 68-82

Guéron, M., Eisinger, J. and Shulman, R.G. (1967) *J. Chem. Phys.* 47, 4077-4091

Heath, O.V.S. (1969) in *The Physiological Aspects of Photosynthesis* Stanford Univ. Press, Stanford

Hoch, G. and Knox, R.S. (1968) in *Photophysiology*, Vol. 3, (Giese, A.C. ed.), Academic Press, New York

Hochstrasser, R.M., and Kasha, M. (1964) *Photochem. Photobiol.* 3, 317-331

Hoff, A.J. (1974) *Photochem. Photobiol.* 19, 51-57

Honssier, C. and Sauer, K. (1970) *J. Am. Chem. Soc.* 92, 779-791

Jackson, J.D. (1962) *Classical Electrodynamics*, Wiley, New York

Katsuura, K. (1964) *J. Chem. Phys.* 40, 3527-3530

Katz, J.J. (1973) *Naturwissenschaften*, 60, 32-39

Kenkre, V.M. and Knox, R.S. (1974) *Phys. Rev. B*, 9, 5279-5290

(1974) *Phys. Rev. Lett.* 33, 803-806

Knapp, A.W. (1965) *J. Math. Anal. Appl.* 12, 328-349

Knox, R.S. (1968) *J. Theoret. Biol.* 21, p. 244

Kreutz, W. (1970) *Adv. Bot. Res.* 3, 53-169

Levine, R.P. (1969) *Sci. Am.* p. 58

McRae and Kasha, M. (1964) in *Physical Processes in Radiation Biology* pp. 23, Academic Press, New York

Merrifield, R.E. (1963) *Rad. Res.* 20, 154-158

Montroll, E.W. (1969) *J. Math. Phys.* 10, 753-765

Muller, A., Lumry, R., Walker, M.S. (1969) *Photochem. Photobiol.* 9, 113-126

- Murrell, J. (1963) The Theory of the Electronic Spectra of Organic Molecules London
- Pearlstein, R.M. (1964) Proc. Nat. Acad. Sci. 52, 824-83
- Rabinovitch, E. and Govindjee (1969) in Photosynthesis, Wiley, New York
- Robinson, G.W. (1967) Brookhaven Natl. Lab. Symp. 19, 16-18
- Schiff, L.I. (1968) Quantum Mechanics, McGraw-Hill, New York
- Schmid, G.H. and Gaffron, H. (1968) J. Gen. Physiol. 52, 212-239
- (1969) Prog. Photosynthesis Res. 2, 857-870
- (1971) Photochem. Photobiol. 14, 451-464
- Siebart, M. and Alfano, R.R. (1974) Biophys. J. 14, 169-283
- Simpson, W.T. and Peterson, D.L. (1957) J. Chem. Phys. 26, 588-593
- Steinemann, A., Stark, G. and Lauger, P. (1972) J. Membrane Bio. 9, 177-194
- Thomas, J.B., Minnaert, K. and Elbers, P.F. (1955) Acta Bot. Neerl. 5, 315-321
- Wolken, J.J. and Schwertz, F.A. (1953) J. Gen. Physiol. 37, 111-119
- Zwanzig, R. (1964) Physica 30, 1109-1123
- (1961) In Lectures in Theoretical Physics, vol. III (Britton, Downs, and Downs, eds.) pp. 106-141 Interscience, New York

APPENDIX A: Derivation of the Forster Equation

Consider two molecules, "a" excited and "b" unexcited, initially. Both molecules may be of the same kind or different. Their total vibronic energies shall be called E'_a and E_b respectively. Excited states will be denoted by prime marks. We shall follow the development with time of situations resulting in molecule "b" excited instead of "a" and where the vibronic energies are then E_a and E'_b respectively. Such a process can be described as :

$$\langle E'_a | \langle E_b | \rightarrow \langle E_a | \langle E'_b |$$

or

$$\langle E'_a, E_b | \rightarrow \langle E_a, E'_b |$$

We normalize the states according to the following prescriptions:

(Dexter, 1953)

$$\langle E'_a | E'_a \rangle = 1 = \langle E_b | E_b \rangle$$

for the initial states, and:

$$\langle E_a | E_a \rangle = \left. \frac{dV_a}{dE} \right|_{E_a}$$

$$\langle E'_b | E'_b \rangle = \left. \frac{dV_b}{dE} \right|_{E'_b}$$

for the final states.

The integrations are over electronic and nuclear coordinates and v_a, v_b' are the quantum members of intramolecular vibration.

With these definitions the orthonormalization relations for different energy states are:

$$\langle E_a | E_a' \rangle = \delta(E_a - E_a') = \left. \frac{dv_a}{dE} \right|_{E_a} \delta(v_a - v_a')$$

$$\langle E_b | E_b' \rangle = \delta(E_b - E_b') = \left. \frac{dv_b}{dE} \right|_{E_b} \delta(v_b - v_b')$$

where we have used the property of the delta function

$$\delta\{g(x)\} = \sum_i \frac{1}{g'(x_i)} \delta(x - x_i)$$

The expectation value of any operator is, from the normalization relations:

$$\langle A \rangle = \langle n | A | n \rangle \frac{dE}{dv}$$

The quantity, $\langle n | A | n \rangle$ represents the density of this expectation value on the energy scale (ie)

$$\langle n | A | n \rangle = \langle n \rangle \frac{dv}{dE}$$

The expectation value itself for any final state energy interval is obtained by integration over this interval.

The corresponding time dependent wave function can be written as a linear combination of the initial and final states:

$$\psi(t) = c_0(t) \psi_{a'b}(E_a', E_b) e^{-\frac{i}{\hbar}(E_a' + E_b)t} + \iint c(E_a, E_b', t) \psi_{ab'}(E_a, E_b') e^{-\frac{i}{\hbar}(E_a + E_b')t} dE_a dE_b' \dots\dots\dots(1)$$

where, $\psi_{ab'} \equiv \langle r | E_a, E_b' \rangle$

We have integrated over all possible final states.

This is a solution of the time-dependant Schroedinger wave equation:

$$i\hbar \frac{d\psi}{dt} = (H_0 + U)\psi \quad (2)$$

where: H_0 is the unperturbed hamiltonian

U is the interaction potential

The coulomb interaction between a and b', and b' and a is included in H_0 . Therefore $\psi_{a'b}$ and $\psi_{ab'}$ are eigenfunctions of H_0

U is only the resonance interaction between the initial and final

states. ie) $\langle E_a', E_b | U_{ab} | E_a, E_b' \rangle$

Substituting Eqn 1 into Eqn 2 and using the initial conditions:

$$C_0(0) = 1 \quad ; \quad C(E_a, E_b', t) = 0$$

gives:

$$\begin{aligned} \frac{dC_0}{dt} \psi_{a'b} e^{-i/\hbar (E_a' + E_b) t} + \iint \frac{dC(E_a, E_b')}{dt} \psi_{a'b} e^{-i/\hbar (E_a + E_b') t} dE_a dE_b' \\ = -\frac{i}{\hbar} U \psi_{a'b} e^{-i/\hbar (E_a' + E_b) t} \end{aligned}$$

We assume all along that no population depletion of the original state occurs.

Multiplying through by ψ^* and integrating using the ortho-normality conditions gives:

$$\frac{dC(E_a, E_b', t)}{dt} = -\frac{i}{\hbar} \langle E_a', E_b | U | E_a, E_b' \rangle e^{-i/\hbar \{ (E_a' + E_b) - (E_a + E_b') \} t} \dots\dots (3)$$

The exponent,

$$(E_a' + E_b) - (E_a + E_b') \equiv (E_a' - E_a) - (E_b' - E_b) \equiv \Delta E$$

is the energy difference between the initial and final states.

The matrix element $U(E_a, E_b')$ is:

$$U(E_a, E_b') \equiv \langle E_a', E_b | U | E_a, E_b' \rangle$$

where the dependence on the initial energies E_a' and E_b' is dropped because these are considered to be constant. (see Eqn 1).

$U(E_a, E_b')$ is the density of the resonance interaction matrix in the (E_a, E_b') plane according to our normalization prescription.

To solve for $C(E_a, E_b', t)$ integrate Eqn 3 using the initial condition: $C(E_a, E_b', 0) = 0$. This leads to

$$C(E_a, E_b', t) = U(E_a, E_b') \frac{e^{-i/\hbar \Delta E t} - 1}{\Delta E}$$

The expectation value for the state $\psi_{a,b'}(E_a, E_b', t)$ then becomes:

$$|C(E_a, E_b', t)|^2 = \frac{4 U^2(E_a, E_b')}{(\Delta E)^2} \sin^2 \left(\frac{\Delta E t}{2\hbar} \right)$$

Since this is a density in energy space, we can integrate over the final state energies E_a and E_b' to obtain the probability, $f_{ab'}$, that molecule "b" is excited, independent of the final vibronic energies of both:

$$\begin{aligned} f_{ab'}(t) &= \iint |C(E_a, E_b', t)|^2 dE_a dE_b' \\ &= 4 \iint \frac{U^2(E_a, E_b') \sin^2 \frac{\Delta E t}{2\hbar}}{(\Delta E)^2} dE_a dE_b' \end{aligned}$$

....(4)

For very-weak coupling limit we can consider Eqn 1 for large times, $t \rightarrow \infty$. In this case we use the fact:

$$\delta(x) = \lim_{t \rightarrow \infty} \frac{\sin^2 tx}{\pi t x^2}$$

So that the limiting value of the integral, Eqn 4, becomes:

$$\begin{aligned} \rho_{ab'}(t) &= \frac{\pi t}{\hbar^2} \iint u^2(E_a, E_{b'}) \delta\left(\frac{\Delta E}{2\hbar}\right) dE_a dE_{b'} \\ &= \frac{2\pi t}{\hbar} \iint u^2(E_a, E_{b'}) \delta(\Delta E) dE_a dE_{b'} \end{aligned} \tag{5}$$

Make the following change of variables:

$$\Delta E = E_{a'} - E_a - E_{b'} + E_b$$

and
$$E = \frac{1}{2} (E_{a'} - E_a + E_{b'} - E_b)$$

Eqn 5 becomes:

$$\rho_{ab'}(t) = \frac{2\pi t}{\hbar} \int u^2(E,0) dE \quad (6)$$

The transfer rate is then:

$$\eta_{a \rightarrow b} = \frac{2\pi}{\hbar} \int u^2(E,0) dE \quad (7)$$

We now turn to the problem of specifying $u(E,0)$. If we return to the original energy parameters, E_a' and E_b then $u(E,0)$ becomes:

$$u(E,0) = u(E_a', E_b; E_a, E_b') = u(E_a', E_b; E_a' - E, E_b + E) \quad \dots(8)$$

E is the amount of energy transferred between the two molecules, therefore the final state energies are expressed here in terms of the original state energies and the transfer energy E .

For simplicity we make the Born-Oppenheimer approximation

$$\begin{aligned} \psi_{a'b}(E_a', E_b) &= \phi_a' \phi_b \chi_a'(E_a') \chi_b(E_b) \\ \psi_{ab'}(E_a, E_b') &= \phi_a \phi_b' \chi_a(E_a - E) \chi_b'(E_b + E) \end{aligned} \quad (9)$$

where χ_l and χ_l' are the vibrational wave functions of the excited and unexcited molecule l . ϕ_l and ϕ_l' are the electronic wave functions. The square of the matrix element $u(E,0)$ in Eqn 8 then becomes Eqn 10

for electronically allowed interactions, neglecting vibrational terms (interaction Hamiltonian is a function of a electronic coordinates only and thus factors out of the integral).

$$\begin{aligned}
 U^2(E, 0) &= \langle \phi_a' \phi_b | V | \phi_a \phi_b' \rangle S_a^2(E_a', E_a' - E) S_b^2(E_b, E_b + E) \\
 &= U^2 S_a^2(E_a', E_a' - E) S_b^2(E_b, E_b + E) \dots (10)
 \end{aligned}$$

where V is the electronic interaction energy and U is the electronic interaction matrix element. S_a and S_b are the vibrational overlap integrals:

$$S_l(E_1, E_2) = \langle \chi_l'(E_1) | \chi_l(E_2) \rangle$$

The next step is to specify the interaction U . We will restrict it to dipole-dipole interaction:

$$\begin{aligned}
 U &= \frac{1}{n^2 R_{ab}^3} \left[\vec{m}_a \cdot \vec{m}_b - \frac{3}{R^2} (\vec{m}_a \cdot \vec{R}_{ab})(\vec{m}_b \cdot \vec{R}_{ab}) \right] \\
 &= \frac{|\vec{m}_a| |\vec{m}_b|}{n^2 R_{ab}^3} K \dots (11)
 \end{aligned}$$

where the terms are defined in Sect. V by Eqn V-3 and V-4.

Inserting Eqn 11 and 10 into Eqn 7 gives:

$$\begin{aligned}
 \eta_{a \rightarrow b}(E_a', E_b) &= \frac{K^2}{n^4 \hbar^2 R_{ab}^6} \int |\vec{m}_a|^2 S_a^2(E_a', E_a' - \hbar\nu) \\
 &\quad \cdot |\vec{m}_b|^2 S_b^2(E_b, E_b + \hbar\nu) d\nu
 \end{aligned}$$

where we have replaced the transfer energy, E by the transfer frequency $\nu = \frac{E}{2\pi\hbar}$, and the integration over energy to integration over frequency.

This is the transfer rate for molecules with the initial states E_a' and E_b . We now introduce the condition of thermal equilibrium in the initial state before energy transfer by the introduction of suitable Boltzmann factors. The total transfer is then just the integration over all energies weighted by these factors, which are continuous functions $g'(E)$ for the excited molecule and $g(E)$ for the unexcited one. Thus we get:

$$\eta_{a \rightarrow b} = \frac{\kappa^2}{h^4 \hbar^2 R_{ab}'} \int \left\{ |m_a|^2 \int g'(E_a') S_a^2(E_a, E_a' - h\nu) dE_a' \right\} \times \left\{ |m_b|^2 \int g(E_b) S_b^2(E_b, E_b + h\nu) dE_b \right\} d\nu \quad (12)$$

The terms in the curly brackets are closely related to spectroscopic transition probabilities between the ground state and excited states of molecules a and b. The first bracket is proportional to the spectral density of the emission spectrum of molecule a at thermal equilibrium in its excited state, i.e. the fluorescence spectrum. The second bracket is proportional to the spectral density of molecule b. The integral in Eqn 12 is then proportional to the overlap integral of the fluorescence spectrum of a with the absorption spectrum of b.

If $\mathcal{E}(\nu)$ and $f(\nu)$ are the emission and absorption intensities respectively, then the following relations can be derived from the Einstein coefficients for absorption and spontaneous emission.

$$\mathcal{E}(\nu) = \frac{2^2 \pi^2 N' |\bar{m}|^2 \nu}{3 (\ln 10) n \hbar c} \int g(E) S^2(E, E + h\nu) dE \quad (13)$$

$$f(\nu) = \frac{2^5 \pi^3 n \tau_e |\bar{m}|^2 \nu^3}{3 \hbar c^3} \int g'(E') S^2(E', E' - h\nu) dE'$$

See Dexter (1953) for a derivation.

N' is the molecular concentration; c is the velocity of light; τ_e is the intrinsic fluorescence lifetime in the absence of quenching processes. Insertion of Eqn 13 into Eqn 12 gives:

$$\eta_{a \rightarrow b} = \frac{1}{\tau_0} \frac{1}{R'_{ab}} \left(\frac{9 \kappa^2 (\ln 10) c^4}{128 \pi^5 n^4 N'} \right) \cdot \int f(\nu) \mathcal{E}(\nu) \frac{d\nu}{\nu^4}$$

This is the Forster equation. It can also be derived on a classical basis by considering molecule b as a dipole in the "near zone" of the oscillating electric field of dipole a. (Hoch and Knox, 1968)

APPENDIX B: DERIVATION OF THE GENERALIZED MASTER EQUATION

The derivation presented here is based on Zwanzig (1964).
The master equation that we are concerned with is a kinetic equation for the diagonal elements of a density matrix. (Schiff, 1968)

Let the density operator be $\hat{\rho}$ and its matrix elements in some representation be ρ_{mn} .

The time dependence of the density matrix is given by von Neumann's equation:

$$\frac{d\hat{\rho}}{dt} = -\frac{i}{\hbar} [\hat{H}, \hat{\rho}] \quad (1)$$

H is the Hamiltonian. As a matrix equation this is:

$$\frac{d\rho_{mn}}{dt} = -\frac{i}{\hbar} \sum_r (H_{mr} \rho_{rn} - \rho_{mr} H_{rn}) \quad (2)$$

We wish to extract an equation giving the time dependence of the diagonal elements of $\hat{\rho}$, which does not contain non-diagonal elements.

Introduce the operator C defined as the commutator:

$$\hat{C} \equiv [\hat{H}, \hat{A}] \quad (3)$$

Define the "Liouville operator" as the operation of going from A to C:

$$\hat{C} = \mathcal{L} \hat{A} \quad (4)$$

In the chosen representation it turns a matrix with two subscripts into another matrix and is represented as a "tetradic", (what a dyad is to second rank tensor).

$$C_{mn} = \sum_{m'} \sum_{n'} L_{mm'n'n'} A_{m'n'} \quad (5)$$

With \mathcal{L} defined as in Eqn 3, the explicit form of the Tetradic is

$$L_{mm'n'n'} = H_{mm'} \delta_{nn'} - \delta_{mm'} H_{n'n} \quad (6)$$

In Liouville operator notation, von Neumann's equation is:

$$\frac{d\hat{\rho}}{dt} = -\frac{i}{\hbar} \mathcal{L}\hat{\rho} \quad (7)$$

It has the solution:

$$\hat{\rho}(t) = e^{-i/\hbar \mathcal{L}t} \hat{\rho}(0)$$

The tetradic operator $\exp(-it\mathcal{L})$ can also be written in terms of the more familiar time evolution operator, $\exp(-itH)$, giving the following useful identity, verified by differentiation with time and application of Eqn 6:

$$\left(e^{-it\mathcal{L}} \right)_{mm'n'n'} = \left(e^{-itH} \right)_{mm'} \left(e^{+itH} \right)_{n'n'} \quad (8)$$

By applying this to Eqn 8 we get the Heisenberg solution:

$$\hat{p}(t) = e^{-it\hat{H}} \hat{p}(0) e^{it\hat{H}}$$

The Laplace transform of \hat{p} is denoted by $g(p)$:

$$\hat{g}(P) = \int_0^{\infty} e^{-Pt} \hat{p}(t) dt \quad (9)$$

On transforming Eqn 7 we get:

$$P \hat{g}(P) - \hat{p}(0) = -\frac{c}{\hbar} \mathcal{L} \hat{g}(P) \quad (10)$$

which has the formal operator solution:

$$\hat{g}(P) = \frac{1}{P + \frac{c}{\hbar} \mathcal{L}} \hat{p}(0) \quad (11)$$

The advantage of introducing \mathcal{L} rather than working with \hat{H} is that the analysis in terms of the Laplace transform is so simple. (Zwanzig, 1964)

To select the diagonal part of \hat{p} , define the projection operator D which in tetradic form is:

$$(D \hat{p})_{mn} = p_{mn} \delta_{mn}$$

$$D_{mnm'n'} = \delta_{mn} \delta_{m'n'} \delta_{nn'} \quad (12)$$

It obeys the fundamental requirement of projection operators:

$$D^2 = D$$

The non-diagonal part is selected by $(1-D)$.

Thus the density operator separates into a diagonal part $\hat{\rho}_1$ and a non-diagonal part: $\hat{\rho}_2$

$$\begin{aligned}\hat{\rho} &= \hat{\rho}_1 + \hat{\rho}_2 \\ \hat{\rho}_1 &= D \hat{\rho} \\ \hat{\rho}_2 &= (1-D) \hat{\rho}\end{aligned}$$

In just the same way, the Laplace transform \hat{g} separates into diagonal and non-diagonal parts:

$$\begin{aligned}\hat{g}(P) &= \hat{g}_1(P) + \hat{g}_2(P) \\ g_1 &= D \hat{g} \\ g_2 &= (1-D) \hat{g}\end{aligned}$$

Next we use D and $(1-D)$ to separate Eqn 10 into two parts:

$$\begin{aligned}D P \hat{g}(P) - D \hat{p}(0) &= -\frac{i}{\hbar} D L \hat{g}(P) \\ (1-D) P \hat{g}(P) - (1-D) \hat{p}(0) &= -\frac{i}{\hbar} (1-D) L \hat{g}(P)\end{aligned}$$

or:
$$P \hat{g}_1(P) - \hat{f}_1(0) = -\frac{i}{\hbar} D \mathcal{L} \hat{g}_1(P) - \frac{i}{\hbar} D \mathcal{L} \hat{g}_2(P)$$

$$P \hat{g}_2(P) - \hat{f}_2(0) = -\frac{i}{\hbar} (1-D) \mathcal{L} \hat{g}_1(P) - \frac{i}{\hbar} (1-D) \mathcal{L} \hat{g}_2(P)$$

...(13)

Solve the second equation for $\hat{g}_2(P)$:

$$\hat{g}_2 = \frac{1}{P + i(1-D)\mathcal{L}} \hat{f}_2(0) - \frac{1}{P + i(1-D)\mathcal{L}} i(1-D)\mathcal{L} \hat{g}_1(P)$$

...(14)

and substitute into the first one

$$P \hat{g}_1(P) - \hat{f}_1(0) = -\frac{i}{\hbar} D \mathcal{L} \hat{g}_1(P) - \frac{i}{\hbar} D \mathcal{L} \frac{1}{P + i(1-D)\mathcal{L}} \hat{f}_2(0) - D \mathcal{L} \frac{1}{P + i(1-D)\mathcal{L}} (1-D) \mathcal{L} \hat{g}_1(P)$$

Invert the transform using the theorem that the inverse of a product is a convolution. The result is:

$$\frac{d\hat{f}_1(t)}{dt} = -i D \mathcal{L} \hat{f}_1(t) - i D \mathcal{L} e^{-i(1-D)\mathcal{L}t} \hat{f}_2(0) - \int_0^t dt_1 D \mathcal{L} e^{-it_1(1-D)\mathcal{L}} (1-D) \mathcal{L} \hat{f}_1(t-t_1)$$

(15)

In most applications of the master equation, the density matrix is initially diagonal, or $\hat{f}_2(0) = 0$. This initial condition is referred to as the assumption of random phases. When it applies,

Eqn 15 makes no reference to the non-diagonal elements of $\hat{\rho}$. Thus the master equation has the desired property of containing only the diagonal elements of $\hat{\rho}$.

When a more general initial condition applies, all of Eqn 15 must be used. Even so, the non-diagonal elements enter only in the initial condition. We will only consider the diagonal elements.

Eqn 15 is expressed in abstract operator notation. We will rewrite it in a more explicit subscript notation. For this we use Eqns. B6 and B12. Choose a representation that diagonalizes the unperturbed Hamiltonian.

$$(H_0)_{mn} = E_m \delta_{mn}$$

Then the unperturbed Liouville operator is:

$$(L_0)_{mm'n'n'} = (E_m - E_n) \delta_{mm'} \delta_{nn'}$$

then

$$DL_0 = L_0D = 0$$

Also the product DLD vanishes for any Hamiltonian. This is seen from the definitions, which lead to:

$$(DL_0D)_{mm'n'n'} = \delta_{mn} L_{mm'm'm'} \delta_{m'n'}$$

But because of Eqn 6, L_{mnn} vanishes and we have:

$$DL D = 0 \quad (16)$$

Eqn 16 serves to eliminate the first term on the right of Eqn 15. The reason is that: $DR\hat{p}_1 = DLD$

The rest of Eqn 15 without the initial value $\hat{p}_2(0)$ has the explicit form:

$$\frac{d p_{mn}(t)}{dt} = - \int_0^t dt_1 [\hat{w}(t_1) \hat{p}_1(t-t_1)]_{mn} \quad (17)$$

where: $\hat{w}(t) = DR e^{-it(1-D)R} (1-D)R \quad (18)$

Because \hat{p}_1 is diagonal, Eqn 17 is:

$$\frac{d p_{mn}(t)}{dt} = - \int_0^t dt_1 \sum_n w_{mnn}(t_1) p_{nn}(t-t_1) \quad (19)$$

Because $D1_i = D_i^0$ the kernel w_{mnn} can be simplified to:

$$w_{mnn}(t) = \left\{ \mathcal{L}_i e^{-it(1-D)R} (1-D)R_i \right\}_{mnn} \quad (20)$$

Next we use the result:

$$\sum_n w_{mnn}(t) = 0 \quad \text{and} \quad \sum_m w_{mnn}(t) = 0$$

This is easily proved by the following demonstration:

$$\begin{aligned} \sum_m w_{mnn} &= \sum_m \sum_a \sum_b (\mathcal{L}_i)_{mmab} \times [\mathcal{L}_i e^{-it(1-D)\mathcal{L}} (1-D)]_{abnn} \\ &= \sum_m (\mathcal{L}_i)_{mmab} \times \left\{ \sum_a \sum_b [\mathcal{L}_i e^{-it(1-D)\mathcal{L}} (1-D)]_{abnn} \right\} \end{aligned}$$

But from Eqn 6: $\sum_m (\mathcal{L}_i)_{mmab} = \sum_m (H_i)_{ma} \delta_{mb} - \sum_m \delta_{ma} (H_i)_{bm}$

$$\begin{aligned} &= (H_i)_{ab} - (H_i)_{ba} \\ &= 0 \end{aligned}$$

which proves our assertion.

We also note that tetrads behave very much like ordinary matrices. In fact their algebra can be reduced to that of matrices by the following trick. In representing an operator by a matrix, we pick some arbitrary ordering of pairs of subscripts so that the pair, (m,n) is denoted by α . In this way Eqn 20 becomes:

$$w_{\alpha\beta}(t) = \left\{ \mathcal{L}_i e^{-it(1-D)\mathcal{L}} (1-D) \mathcal{L}_i \right\}_{\alpha\beta} \quad (20a)$$

and the sum rule becomes: $\sum_{\alpha} w_{\alpha\beta} = 0$

Eqn 19 becomes:

$$\frac{d\rho_{\alpha}}{dt} = - \int_0^t dt' \cdot \sum_{\beta} w_{\alpha\beta}(t') \rho_{\beta}(t-t') \quad (19a)$$

Using the sum rule we can write the integrand in Eqn 19a as:

$$\begin{aligned} \sum_{\beta} w_{\alpha\beta}(t') \rho_{\beta}(t-t') &= \sum_{\beta} w_{\alpha\beta}(t') \rho_{\beta}(t-t') - \rho_{\alpha} \sum_{\beta} w_{\beta\alpha} \\ &= \sum_{\beta} \{w_{\alpha\beta}(t') \rho_{\beta}(t-t') - w_{\beta\alpha} \rho_{\alpha}(t-t')\} \end{aligned}$$

Thus Eqn 19a becomes:

$$\frac{d\rho_{\alpha}}{dt} = - \int_0^t dt' \sum_{\beta} \{w_{\alpha\beta}(t-t') \rho_{\beta}(t-t') - w_{\beta\alpha}(t-t') \rho_{\alpha}(t-t')\} \quad \dots(21)$$

where $w_{\alpha\beta}$ is defined by Eqn 20a.

In the representation of the unperturbed Hamiltonian where $\langle \alpha |$ and $\langle \beta |$ are eigenstates of H then:

$$P_{\alpha} \equiv \langle \alpha | \rho | \alpha \rangle$$

is the diagonal element of ρ in the representation of H_0 eigenstates. It represents the probability of occupancy of the state α .

Thus Eqn 21 becomes:

$$\frac{dP_{\alpha}(t)}{dt} = - \int_0^t dt' \sum_{\beta} \{w_{\alpha\beta}(t-t') P_{\beta}(t-t') - w_{\beta\alpha}(t-t') P_{\alpha}(t-t')\} \quad \dots(22)$$

This is the generalized master equation for the transport of excitation in the familiar gain-loss form. The physical meaning of Eqn 22 is discussed in Sect. IV.

APPENDIX C: Derivation of the memory Function for
Molecular transistions

In appendix B we derived the operator form of the memory function, Eqn B20a:

$$\hat{w}(t) = D \mathcal{L} e^{-it(1-D)} \mathcal{R} (1-D) \mathcal{L} \quad (1)$$

We will now derive an explicit form for this equation for molecular systems. \mathcal{L} is the Liouville operator defined by:

$$\mathcal{L} \hat{A} \equiv [\hat{H}, \hat{A}] \equiv \hat{H} \hat{A} - \hat{A} \hat{H}$$

\hat{A} is an operator and \hat{H} is the Hamiltonian. D is a projection operator that selects the diagonal part of whatever it operates on:

$$D \hat{A} = \hat{A}_d$$

where \hat{A}_d is the diagonal part of \hat{A} ,

and \hat{W} is the basic quantity in the GME approach.

It connects the probability at a site α at time in the past to the rate change of the probability at site β in the present time t .

We will start from Eqn B17:

$$\frac{d \hat{\rho}_{mm}(t)}{dt} = - \int_0^t [w(t_1) \rho_d(t_1)]_{mm} dt_1 \quad (2)$$

where ρ_{mm} is the diagonal part of the density matrix.

Eqn B20a can easily be written, by definition of D as:

$$D(\mathcal{L} e^{-it(1-D)\mathcal{L}} (1-D)\mathcal{L} \rho_d) = \{ \mathcal{L} e^{-it(1-D)\mathcal{L}} (1-D)\mathcal{L} \rho_d \}_{\alpha, \alpha}$$

and by the definition of L as:

$$\mathcal{L} \{ e^{-it(1-D)\mathcal{L}} (1-D)\mathcal{L} \} = \frac{1}{\hbar} [H_1 e^{-it(1-D)\mathcal{L}} (1-D)\mathcal{L} \rho_d]$$

Because $\hat{H} = \hat{H}_0 + \hat{H}'$ with \hat{H}_0 diagonal, the commutator with becomes zero and we are left with:

$$\frac{1}{\hbar} [H', e^{-it(1-D)\mathcal{L}} (1-D)\mathcal{L} \rho]_{\alpha, \alpha} \quad (3)$$

Next we note that:

$$e^{-it(1-D)\mathcal{L}} (1-D) = [e^{-it\mathcal{L}_0} + (\text{higher order})](1-D)$$

Neglecting higher order terms we get using Eqn B8 :

$$e^{-it\mathcal{L}_0} (1-D) \rho = e^{-iH_0 t/\hbar} [(1-D)\mathcal{L} \rho] e^{iH_0 t/\hbar}$$

Putting this back into Eqn 3

$$\frac{1}{\hbar} \left[H', e^{-iH_0 t/\hbar} (1-D) \mathcal{L} p e^{-iH_0 t/\hbar} \right]_{\alpha\alpha}$$

Next we use the result:

$$(1-D) \mathcal{L} p_d = \frac{1}{\hbar} (1-D) [H, p_d] = \frac{1}{\hbar} [H', p]$$

because $[H_0, p] = 0$

This gives:

$$\frac{1}{\hbar^2} \left[H', e^{-iH_0 t/\hbar} [H', p_d] e^{iH_0 t/\hbar} \right]_{\alpha\alpha}$$

The result can be completely written in Matrix form as:

$$\frac{2}{\hbar^2} \sum_{\alpha \neq \beta} |H'_{\alpha\beta}|^2 \cos \frac{(E_\alpha - E_\beta)t}{\hbar} \left\{ p_{\alpha\alpha}(t-s) - p_{\beta\beta}(t-s) \right\}$$

using the definitions of the elements as:

$$\langle \alpha | H_0 | \alpha \rangle = E_\alpha$$

$$\langle \alpha | H_0 | \beta \rangle = 0$$

$$\langle \alpha | H' | \beta \rangle = H_{\alpha\beta}$$

from which we can define $W_{\alpha\beta}$ in Eqn B22 as:

$$W_{\alpha\beta}(t) = \frac{2}{\hbar^2} |H'_{\alpha\beta}|^2 \cos \left(\frac{E_\alpha - E_\beta}{\hbar} t \right) \quad (4)$$

Inspection of Eqn 2 shows that the basic microscopic form of W is oscillatory and non-decaying. A irreversible description of excitation transport and the possible transition to the Pauli equation necessitates a decaying memory, in order to account for the loss of coherence or phase correlation between excitation at one site and an earlier site. We should obtain a delta function in the appropriate limit. To obtain a decaying memory one requires a coarse graining operation representing the passage from microscopic to macroscopic level of description. Coarse graining means taking an average over small regions of the state space. If the microscopic states are α, β then the macroscopic coarse-grained states are an average of α, β in some small region of the state space. This coarse -graining in terms of molecular transistions would mean averaging over the vibrational states of a particular electronic transition.

We can write the coarse-grained w as follows:

$$W_{\alpha'\beta'}(t) = \frac{2}{\hbar^2} \sum_{\{\alpha, \beta\} \in \{\alpha', \beta'\}} |H_{\alpha\beta}|^2 \cos \frac{(E_\alpha - E_\beta)t}{\hbar} \quad (5)$$

Compare this with Eqn 4 above.

Using this w , the GME would describe transport in the coarse-grained space of the $\alpha'\beta'$ states.

If we let: $|\alpha\rangle = |\alpha'\rangle |a\rangle$

which is appropriate when the description is in terms of a thermal bath whose states are $|a\rangle$, then Eqn 5 becomes (Knox and Kenkre, 1974),

$$W_{\alpha'\beta'}(t) = \frac{2}{\hbar} \sum_{a,b} |H_{ab}|^2 \cos(\omega_{ab}t) \cos(\Omega_{\alpha'\beta'}t) \quad (6)$$

where: $|H_{ab}|^2 = |\langle \alpha' | \langle a | V | b \rangle | \beta' \rangle|^2$

$$\omega_{ab} = (E_a - E_b) / \hbar$$

$$\Omega_{\alpha'\beta'} = (E_{\alpha'} - E_{\beta'}) / \hbar$$

$\Omega_{\alpha'\beta'}$ is the energy difference of the coarse grained system and ω_{ab} is the energy differences of the bath states. The transition probability with memory $W_{\alpha'\beta'}$ is thus seen to emerge (except for the $\cos(\Omega t)$ factor) as the Fourier transform of the interaction:

$$|\langle \alpha', a | V | \beta', b \rangle|^2$$

Thus the decaying memory arises out of the basic oscillatory memory at the microscopic level.

The Förster equation involves the interaction energy in coarse grained space because it averages over a Boltzmann weighted distribution of states. (Eqn A12) Knox and Kenkre (1974) slightly modify the derivation presented in Appendix A so as to include a $\cos(\omega t)$ factor and integration over all possible ω as required by Eqn 6 (Summations become integrals for the continuum of states assumed in the derivation of the Förster equation.) ω represents all possible differences in energy between states of the "bath". Their result is:

$$w_{mn}(t) = \frac{1}{\pi} \int_{-\infty}^{\infty} F_{mn}(\omega) \cos(\omega t) d\omega$$

where: $F_{mn}(\omega)$ is the Förster equation for the transition rate between molecules m and n as a function of the variable ω which represents the energy differences of the states of the "bath".

A physical interpretation of ω in terms of the stokes shift has been given in Sect. IV. $F_{mn}(0)$ represents the normal Förster equation. Factoring out the time dependence, Eqn IV-1 gives:

$$\phi(t) = (\pi F_{mn})^{-1} \int_{-\infty}^{\infty} F_{mn}(\omega) \cos(\omega t) d\omega$$

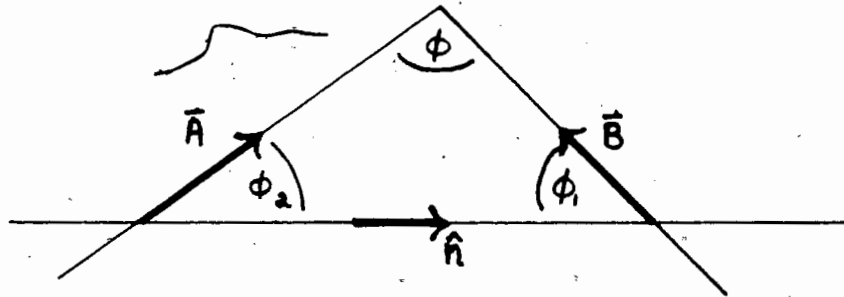
The use of this equation for the memory function is discussed in Section IV.

APPENDIX D: The orientation factor

We have the following relation between two vectors:

$$\bar{A} \cdot \bar{B} - 3(\bar{A} \cdot \hat{n})(\bar{B} \cdot \hat{n}) \equiv \chi$$

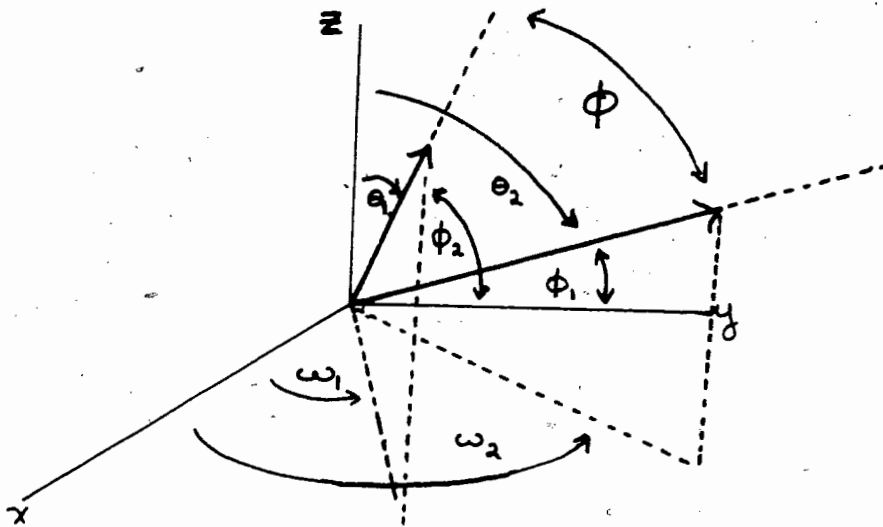
where \hat{n} is the unit vector along the line joining them:



Setting $|\bar{A}| = |\bar{B}| = 1$ the above relationship becomes:

$$\chi = \cos \phi - 3 \cos \phi_1 \cdot \cos \phi_2$$

where the angles are shown in the above diagram. The situation can be represented in spherical polar coordinates as follows:



We wish to find the RMS average of ϕ over all orientations of azimuthal angles ω_1, ω_2 , for fixed polar angles θ_1, θ_2 as follows:

$$\langle \kappa^2 \rangle = \frac{1}{(2\pi)^2} \int_0^{2\pi} \int_0^{2\pi} d\omega_1 d\omega_2 (\cos \phi - 3 \cos \phi_1 \cdot \cos \phi_2)^2 \quad \dots(1)$$

We must write ϕ, ϕ_1, ϕ_2 in terms of $\theta_1, \theta_2, \omega_1, \omega_2$ the polar angles.

Immediately from the diagram we have:

$$\begin{aligned} \cos \phi_1 &= \cos \omega_1 \sin \theta_1 \\ \cos \phi_2 &= \cos \omega_2 \sin \theta_2 \end{aligned} \quad (2)$$

To find a relationship for $\cos \phi$ we use the Addition Theorem for Spherical Harmonics. (Jackson, sect 3.5):

$$P_l(\cos \phi) = \frac{4\pi}{2l+1} \sum_{m=-l}^l Y_{lm}^*(\theta_1, \omega_1) Y_{lm}(\theta_2, \omega_2)$$

which for $l=1$ we obtain:

$$\cos \phi = \sin \theta_1 \sin \theta_2 \cos(\omega_1 - \omega_2) + \cos \theta_1 \cos \theta_2 \quad (3)$$

We let $\theta_1 = \theta_2 = \beta'$ and substitute into Eqn D1:

$$\langle k^2 \rangle = \frac{1}{4\pi^2} \int_0^{2\pi} \int_0^{2\pi} \left\{ \cos^4 \beta' + \sin^4 \beta' (\sin \omega_1 \sin \omega_2 - 2 \cos \omega_1 \cos \omega_2)^2 + 2 \cos^2 \beta' \sin^2 \beta' (\sin \omega_1 \sin \omega_2 - 2 \cos \omega_1 \cos \omega_2) \right\} d\omega_1 d\omega_2$$

The odd sine and cosine terms will integrate to zero.

We are left with:

$$\langle k^2 \rangle = \cos^4 \beta' + \frac{\sin^4 \beta'}{4\pi^2} \times \int_0^{2\pi} \int_0^{2\pi} (\sin^2 \omega_1 \sin^2 \omega_2 + 4 \cos^2 \omega_1 \cos^2 \omega_2) d\omega_1 d\omega_2$$

which is:

$$\langle \kappa^2 \rangle = \cos^4 \beta' + \frac{5}{4} \sin^4 \beta'$$

where β' is the angle perpendicular to the x,y plane (membrane plane).

In terms of the angle with the plane we can write:

$$\beta = 90^\circ - \beta'$$

We have finally the required result:

$$\langle \kappa^2 \rangle = \sin^4 \beta + \frac{5}{4} \cos^4 \beta$$

APPENDIX E: Derivation of the Wave Equation from the
Generalized Master Equation

We wish to show that

$$\frac{dP_i(t)}{dt} = \int_0^t ds \phi(t-s) \left\{ \sum_j (F_{ij} P_j(s) - F_{ji} P_i(s)) \right\}$$

has the form:

$$\frac{\partial P(x,t)}{\partial t} = \int_0^t Q(t-s) \frac{\partial^2 P(x,s)}{\partial x^2} ds$$

The summation in Eqn 1 for nearest neighbours becomes:

$$F_{i,i+1} P_{i+1} - F_{i+1,i} P_i + F_{i,i-1} P_{i-1} - F_{i-1,i} P_i(s)$$

If we assume reversibility and isotropy, i.e.

$$F_{i,i+1} = F_{i+1,i} = F_{i,i-1} = F_{i-1,i}$$

we get

$$F [P_{i+1} - 2P_i + P_{i-1}]$$

This is the difference form of the second differential, so in the continuum limit we have:

$$F \frac{\partial^2 P(x,s)}{\partial x^2}$$

Substituting in Eqn 1 we obtain

$$\frac{\partial P(x,t)}{\partial t} = \int_0^t ds Q(t-s) \frac{\partial^2 P(x,s)}{\partial x^2}$$

where $Q = \phi F$

If we let: $Q(t-s) = k \Theta(t)$

where:

$$\Theta(t) = \begin{cases} 0 & s < 0 \\ 1 & s > 0 \end{cases}$$

then Eqn 3 becomes

$$\frac{\partial P(x,t)}{\partial t} = \int_0^t ds k \Theta(t) \frac{\partial^2 P(x,s)}{\partial x^2} = k \int_0^t ds \frac{\partial^2 P(x,s)}{\partial x^2}$$

which is

$$\frac{\partial^2 P(x,t)}{\partial t^2} = k \frac{\partial^2 P(x,t)}{\partial x^2}$$

This is the wave equation with $k = (\text{velocity})^2$

It is easily seen that substituting

$$Q(t-s) = k \delta(t)$$

gives the diffusion equation.